EUROPEAN ORGANIZATION FOR NUCLEAR RESEARCH (CERN)

CERN-EP-2018-071
2018/12/03

CMS-SMP-16-015

Measurement of differential cross sections for Z boson production in association with jets in proton-proton collisions at $\sqrt{s} = 13\,\text{TeV}$

The CMS Collaboration*

Abstract

The production of a Z boson, decaying to two charged leptons, in association with jets in proton-proton collisions at a centre-of-mass energy of 13 TeV is measured. Data recorded with the CMS detector at the LHC are used that correspond to an integrated luminosity of 2.19 fb^{-1}. The cross section is measured as a function of the jet multiplicity and its dependence on the transverse momentum of the Z boson, the jet kinematic variables (transverse momentum and rapidity), the scalar sum of the jet momenta, which quantifies the hadronic activity, and the balance in transverse momentum between the reconstructed jet recoil and the Z boson. The measurements are compared with predictions from four different calculations. The first two merge matrix elements with different parton multiplicities in the final state and parton showering, one of which includes one-loop corrections. The third is a fixed-order calculation with next-to-next-to-leading order accuracy for the process with a Z boson and one parton in the final state. The fourth combines the fully differential next-to-next-to-leading order calculation of the process with no parton in the final state with next-to-next-to-leading logarithm resummation and parton showering.

Published in the European Physical Journal C as doi:10.1140/epjc/s10052-018-6373-0.

*See Appendix A for the list of collaboration members

1 Introduction

Measurements of vector boson production in association with jets provide fundamental tests of quantum chromodynamics (QCD). The high centre-of-mass energy at the CERN LHC allows the production of an electroweak boson along with a large number of jets with large transverse momenta. A precise knowledge of the kinematic distributions in processes with large jet multiplicity is essential to exploit the potential of the LHC experiments. Comparison of the measurements with predictions motivates additional Monte Carlo (MC) generator development and improves our understanding of the prediction uncertainties. Furthermore, the production of a massive vector boson together with jets is an important background to a number of standard model (SM) processes (production of a single top quark, $\mathrm{t\bar{t}}$, and Higgs boson as well as vector boson fusion and WW scattering) as well as to searches for physics beyond the SM, e.g. supersymmetry. Leptonic decay modes of the vector bosons are often used in the measurement of SM processes and searches for physics beyond the SM since they have a sufficiently high branching fraction and clean signatures that provide a strong rejection of backgrounds. Differential cross sections for the associated production of a Z boson with hadronic jets have been previously measured by the ATLAS, CMS, and LHCb Collaborations in proton-proton collisions at centre-of-mass energies of 7 [1–4], 8 [5–7] and 13 [8] TeV, and by the CDF and D0 Collaborations in proton-antiproton collisions at 1.96 TeV [9, 10].

In this paper, we present measurements of the cross section multiplied by the branching fraction for the production of a Z/γ^* boson in association with jets and its subsequent decay into a pair of oppositely charged leptons ($\ell^+\ell^-$) in proton-proton collisions at a centre-of-mass energy of 13 TeV. The measurements from the two final states, with an electron–positron pair (electron channel) and with a muon–antimuon pair (muon channel), are combined. The measurements are performed with data from the CMS detector recorded in 2015 at the LHC corresponding to 2.19 fb^{-1} of integrated luminosity. For convenience, Z/γ^* is denoted as Z. In this paper a Z boson is defined as a pair of oppositely charged muons or electrons with invariant mass in the range 91 ± 20 GeV. This range is chosen to have a good balance between the signal acceptance, the rejection of background processes, and the ratio of Z boson to γ^* event yields. It is also consistent with previous measurements [4–6] and eases comparisons.

The cross section is measured as a function of the jet multiplicity (N_{jets}), transverse momentum (p_{T}) of the Z boson, and of the jet transverse momentum and rapidity (y) of the first, second, and third jets, where the jets are ordered by decreasing p_{T}. Furthermore, the cross section is measured as a function of the scalar sum of the jet transverse momenta (H_{T}) for event samples with at least one, two, and three jets. These observables have been studied in previous measurements. In addition, we study the balance in transverse momentum between the reconstructed jet recoil and the Z boson for the different jet multiplicities and two Z boson p_{T} regions ($p_{\mathrm{T}}(\mathrm{Z}) < 50$ GeV and $p_{\mathrm{T}}(\mathrm{Z}) > 50$ GeV).

2 The CMS detector

The central feature of the CMS apparatus is a superconducting solenoid of 6 m internal diameter, providing a magnetic field of 3.8 T. Within the solenoid volume are a silicon pixel and strip tracker, a lead tungstate crystal electromagnetic calorimeter (ECAL), and a brass and scintillator hadron calorimeter (HCAL), each composed of a barrel and two endcap sections. Forward calorimeters extend the pseudorapidity coverage provided by the barrel and endcap detectors up to $|\eta| = 5$. The electron momentum is estimated by combining the energy measurement in the ECAL with the momentum measurement in the tracker. The momentum

resolution for electrons with $p_T \approx 45\,\text{GeV}$ from $Z \to ee$ decays ranges from 1.7% for nonshowering electrons in the barrel region ($|\eta| < 1.444$) to 4.5% for showering electrons in the endcaps ($1.566 < |\eta| < 3$) [11]. When combining information from the entire detector, the jet energy resolution is 15% at 10 GeV, 8% at 100 GeV, and 4% at 1 TeV, to be compared to about 40, 12, and 5% obtained when only the ECAL and HCAL calorimeters are used. Muons are measured in the pseudorapidity range $|\eta| < 2.4$, with detection planes made using three technologies: drift tubes, cathode strip chambers, and resistive plate chambers. Matching muons to tracks measured in the silicon tracker results in a relative transverse momentum resolution for muons with $20 < p_T < 100\,\text{GeV}$ of 1.3–2.0% in the barrel and better than 6% in the endcaps. The p_T resolution in the barrel is better than 10% for muons with p_T up to 1 TeV [12].

Events of interest are selected using a two-tiered trigger system [13]. The first level (L1), composed of custom hardware processors, uses information from the calorimeters and muon detectors to select events at a rate of around 100 kHz within a time interval of less than 4 μs. The second level, known as the high-level trigger (HLT), consists of a farm of processors running a version of the full event reconstruction software optimized for fast processing, and reduces the event rate to around 1 kHz before data storage.

3 Observables

The cross section is measured for jet multiplicities up to 6 and differentially as a function of the transverse momentum of the Z boson and as a function of several jet kinematic variables, including the jet transverse momentum, rapidity, and the scalar sum of jet transverse momenta.

Jet kinematic variables are measured for event samples with at least one, two, and three jets. In the following, the jet multiplicity will be referred to as "inclusive" to designate events with at least N jets and as "exclusive" for events with exactly N jets.

The balance between the Z boson and jet transverse momenta is also studied via the p_T balance observable $p_T^{\text{bal}} = |\vec{p}_T(Z) + \sum_{\text{jets}} \vec{p}_T(j_i)|$, and the so-called jet-Z balance JZB $= |\sum_{\text{jets}} \vec{p}_T(j_i)| - |\vec{p}_T(Z)|$, where the sum runs over jets with $p_T > 30\,\text{GeV}$ and $|y| < 2.4$ [14, 15]. The hadronic activity not included in the jets will lead to an imbalance that translates into p_T^{bal} and JZB values different from zero. It includes the activity in the forward region ($|y| > 2.4$), which is the dominant contribution according to simulation. Gluon radiation in the central region that is not clustered in a jet with $p_T > 30\,\text{GeV}$ will also contribute to the imbalance. Hadronic activity not included in the jets will lead to a shift of the p_T^{bal} distribution peak to larger values. The JZB variable distinguishes between two configurations, one where transverse momentum due to the unaccounted hadronic activity is in the direction of the Z boson and another where it is in the opposite direction. Events in the first configuration that have a large imbalance will populate the positive tail of the JZB distribution, while those in the second configuration populate the negative tail.

The distribution of p_T^{bal} is measured for events with minimum jet multiplicities of 1, 2, and 3. To separate low and high jet multiplicity events without p_T and y constraints on the jets, the JZB variable is also studied for $p_T(Z)$ below and above 50 GeV.

The Z boson transverse momentum $p_T(Z)$ can be described via fixed-order calculations in perturbative QCD at high values, while at small transverse momentum this requires resummation of multiple soft-gluon emissions to all orders in perturbation theory [16, 17]. The measurement of the distribution of $p_T(Z)$ for events with at least one jet, due to the increased phase space for soft gluon radiation, leads to an understanding of the balance in transverse momentum be-

tween the jets and the Z boson, and can be used for comparing theoretical predictions that treat multiple soft-gluon emissions in different ways.

4 Phenomenological models and theoretical calculations

The measured Z + jets cross section is compared to four different calculations: two merging matrix elements (MEs) with various final-state parton multiplicities together with parton showering; a third with a combination of next-to-next-to-leading order (NNLO) calculation with next-to-next-to-leading logarithmic (NNLL) resummation and with parton showering; and a fourth with fixed-order calculation.

The first two calculations use MADGRAPH5_aMC@NLO version 2.2.2 (denoted MG5_aMC) [18], which is interfaced with PYTHIA8 (version 8.212) [19]. PYTHIA8 is used to include initial- and final-state parton showers and hadronisation. Its settings are defined by the CUETP8M1 tune [20], in particular the NNPDF 2.3 [21] leading order (LO) parton distribution function (PDF) is used and the strong coupling $\alpha_S(m_Z)$ is set to 0.130. The first calculation includes MEs computed at LO for the five processes $pp \to Z + N$ jets, $N = 0 \ldots 4$ and matched to the parton shower using the k_T-MLM [22, 23] scheme with the matching scale set at 19 GeV. In the ME calculation, the NNPDF 3.0 LO PDF [24] is used and $\alpha_S(m_Z)$ is set to 0.130 at the Z boson mass scale. The second calculation includes MEs computed at NLO for the three processes $pp \to Z + N$ jets, $N = 0 \ldots 2$ and merged with the parton shower using the FxFx [25] scheme with the merging scale set at 30 GeV. The NNPDF 3.0 next-to-leading order (NLO) PDF is used and $\alpha_S(m_Z)$ is set to 0.118. This second calculation is also employed to derive nonperturbative corrections for the fixed-order prediction discussed in the following.

The third calculation uses the GENEVA 1.0-RC2 MC program (GE), where an NNLO calculation for Drell–Yan production is combined with higher-order resummation [26, 27]. Logarithms of the 0-jettiness resolution variable, τ, also known as beam thrust and defined in Ref. [28], are resummed at NNLL including part of the next-to-NNLL (N^3LL) corrections. The accuracy refers to the τ dependence of the cross section and is denoted NNLL$'_\tau$. The PDF set PDF4LHC15 NNLO [29] is used for this calculation and $\alpha_S(m_Z)$ is set to 0.118. The resulting parton-level events are further combined with parton showering and hadronisation provided by PYTHIA8 using the same tune as for MG5_aMC.

Finally, the distributions measured for $N_{\text{jets}} \geq 1$ are compared with the fourth calculation performed at NNLO accuracy for Z + 1 jet using the N-jettiness subtraction scheme (N_{jetti}) [30, 31]. The PDF set CT14 [32] is used for this calculation. The nonperturbative correction obtained from MG5_aMC and PYTHIA8 is applied. It is calculated for each bin of the measured distributions from the ratio of the cross section values obtained with and without multiple parton interactions and hadronisation. This correction is less than 7%.

Given the large uncertainty in the LO calculation for the total cross section, the prediction with LO MEs is rescaled to match the $pp \to Z$ cross section calculated at NNLO in α_S and includes NLO quantum electrodynamics (QED) corrections with FEWZ [33] (version 3.1b2). The values used to normalise the cross section of the MG5_aMC predictions are given in Table 1. All the numbers correspond to a 50 GeV dilepton mass threshold applied before QED final-state radiation (FSR). With FEWZ, the cross section is computed in the dimuon channel, using a mass threshold applied after QED FSR, but including the photons around the lepton at a distance $R = \sqrt{(\Delta\eta)^2 + (\Delta\phi)^2}$ smaller than 0.1. The number given in the table includes a correction computed with the LO sample to account for the difference in the mass definition. This correction is small, +0.35%. When the mass threshold is applied before FSR, the cross

section is assumed to be the same for the electron and muon channels.

Table 1: Values of the pp $\to \ell^+\ell^-$ total cross section used for the calculation in data-theory comparison plots. The cross section used, the cross section from the MC generator ("native"), and the ratio of the two (k) are provided. The phase space of the sample to which the cross section values correspond is indicated in the second column.

Prediction	Phase space	Native cross section [pb]	Calculation	Used cross section [pb]	k
MG5_aMC +PYTHIA8, $\leq$4 j LO+PS	$m_{\ell^+\ell^-} > 50\,\text{GeV}$	1652	FEWZ NNLO	1929	1.17
MG5_aMC +PYTHIA8, $\leq$2 j NLO+PS	$m_{\ell^+\ell^-} > 50\,\text{GeV}$	1977	native	1977	1
GENEVA	$m_{\ell^+\ell^-} \in [50, 150\,\text{GeV}]$	1980	native	1980	1

Uncertainties in the ME calculation (denoted *theo. unc.* in the figure legends) are estimated for the NLO MG5_aMC, NNLO, and GENEVA calculations following the prescriptions recommended by the authors of the respective generators. The uncertainty coming from missing terms in the fixed-order calculation is estimated by varying the normalisation (μ_R) and factorisation (μ_F) scales by factors 0.5 and 2. In the case of the FxFx-merged sample, the envelope of six combinations of the variations is considered, the two combinations where one scale is varied by a factor 0.5 and the other by a factor 2 are excluded. In the case of the NNLO and GENEVA samples the two scales are varied by the same factor, leading to only two combinations. For GENEVA, the uncertainty is symmetrised by using the maximum of the up and down uncertainties for both cases. The uncertainty from the resummation is also estimated and added in quadrature. It is estimated using six profile scales [34, 35], as described in Ref. [26]. Uncertainties in PDF and α_S values are also estimated in the case of the FxFx-merged sample. The PDF uncertainty is estimated using the set of 100 replicas of the NNPDF 3.0 NLO PDF, and the uncertainty in the α_S value used in the ME calculation is estimated by varying it by ± 0.001. These two uncertainties are added in quadrature to the ME calculation uncertainties. For GENEVA and NLO MG5_aMC all these uncertainties are obtained using the reweighting method [26, 36] implemented in these generators.

5 Simulation

MC event generators are used to simulate proton-proton interactions and produce events from signal and background processes. The response of the detector is modeled with GEANT4 [37]. The $Z(\to \ell^+\ell^-)$ + jets process is generated with NLO MG5_aMC interfaced with PYTHIA8, using the FxFx merging scheme as described in Section 4. The sample includes the $Z \to \tau^+\tau^-$ process, which is considered a background. Other processes that can give a final state with two oppositely charged same-flavour leptons and jets are WW, WZ, ZZ, $t\bar{t}$ pairs, and single top quark production. The $t\bar{t}$ and single top quark backgrounds are generated using POWHEG version 2 [38–41] interfaced with PYTHIA8. Background samples corresponding to diboson electroweak production (denoted VV in the figure legends) [42] are generated at NLO with POWHEG interfaced to PYTHIA8 (WW), MG5_aMC interfaced to PYTHIA8 or PYTHIA8 alone (WZ and ZZ). The background sample corresponding to W + jets production (W) is generated at NLO using MG5_aMC interfaced with PYTHIA8, utilizing the FxFx merging scheme.

The events collected at the LHC contain multiple superimposed proton-proton collisions within a single beam crossing, an effect known as pileup. Samples of simulated pileup are generated with a distribution of proton-proton interactions per beam bunch crossing close to that observed in data. The number of pileup interactions, averaging around 20, varies with the beam conditions. The correct description of pileup is ensured by reweighting the simulated sample to match the number of interactions measured in data.

6 Object reconstruction and event selection

The particle-flow (PF) algorithm [43] is used to reconstruct the events. It combines the information from the various elements of the CMS detector to reconstruct and identify each particle in the event. The reconstructed particles are called PF candidates. If several primary vertices are reconstructed, we use the one with the largest quadratic sum of associated track transverse momenta as the vertex of the hard scattering and the other vertices are assumed to be pileup.

The online trigger selects events with two isolated electrons (muons) with transverse momenta of at least 17 and 12 (17 and 8) GeV. After offline reconstruction, the leptons are required to satisfy $p_{\mathrm{T}} > 20\,\mathrm{GeV}$ and $|\eta| < 2.4$. We require that the two electrons (muons) with highest transverse momenta form a pair of oppositely charged leptons with an invariant mass in the range $91 \pm 20\,\mathrm{GeV}$. The transition region between the ECAL barrel and endcap ($1.444 < |\eta| < 1.566$) is excluded in the reconstruction of electrons and the missing acceptance is corrected to the full $|\eta| < 2.4$ region. The reconstruction of electrons and muons is described in detail in Refs. [11, 12]. The identification criteria applied for electrons and muons are identical to those described in the Ref. [6] except for the thresholds of the isolation variables, which are optimised for 13 TeV centre-of-mass energy in our analysis. Electrons (muons) are considered isolated based on the scalar p_{T} sum of the nearby PF candidates with a distance $R = \sqrt{(\Delta\eta)^2 + (\Delta\phi)^2} < 0.3$ (0.4). The scalar p_{T} sum must be less than 15 (25)% of the electron (muon) transverse momentum. We also correct the simulation for differences from data in the trigger, and the lepton identification, reconstruction and isolation efficiencies. These corrections, which depend on the run conditions, are derived using data taken during the run period, and they typically amount to 1–2% for the reconstruction and identification efficiency and 3–5% for the trigger efficiency.

Jets at the generator level are defined from the stable particles ($c\tau > 1\,\mathrm{cm}$), neutrinos excluded, clustered with the anti-k_{T} algorithm [44] using a radius parameter of 0.4. The jet four-momentum is obtained according to the E-scheme [45] (vector sum of the four-momenta of the constituents). In the reconstructed data, the algorithm is applied to the PF candidates. The technique of charged-hadron subtraction [43] is used to reduce the pileup contribution by removing charged particles that originate from pileup vertices. The jet four-momentum is corrected for the difference observed in the simulation between jets built from PF candidates and generator-level particles. The jet mass and direction are kept constant for the corrections, which are functions of the jet η and p_{T}, as well as the energy density and jet area quantities defined in Ref. [46, 47]. The latter are used in the correction of the energy offset introduced by the pileup interactions. Further jet energy corrections are applied for differences between data and simulation in the pileup in zero-bias events and in the p_{T} balance in dijet, Z + jet, and γ + jet events. Since the p_{T} balance in Z + jet events is one of the observables we are measuring in this paper, it is important to understand how it is used in the jet calibration. The balance is measured for events with two objects (jet, γ, or Z boson) back-to-back in the transverse plane ($|\Delta\phi - \pi| < 0.34$) associated with a possible third object, a soft jet. The measurement is made for various values of $\rho = p_{\mathrm{T}}^{\text{soft jet}} / p_{\mathrm{T}}^{\mathrm{ref}}$, running from 0.1 to 0.3, and extrapolated to $\rho = 0$. In the case the back-to-back objects are a jet and a boson, $p_{\mathrm{T}}^{\mathrm{ref}}$ is defined as the transverse momentum of the boson, while in the case of two jets it is defined as the average of their transverse momenta. All jets down to $p_{\mathrm{T}} = 5$ or 10 GeV, including jets reconstructed in the forward calorimeter, are considered for the soft jet. The data-simulation adjustment is therefore done for ideal topologies with only two objects, whose transverse momenta must be balanced. The jet calibration procedure is detailed in the Ref. [48]. In this measurement, jets are further required to satisfy the loose identification criteria defined in Ref. [49]. Despite the vertex requirement used in the jet clustering some jets are reconstructed from pileup candidates; these jets are sup-

pressed using the multivariate technique described in Ref. [50]. Jets with $p_{\mathrm{T}} > 30\,\mathrm{GeV}$ and $|y| < 2.4$ are used in this analysis.

7 Backgrounds estimation

The contributions from background processes are estimated using the simulation samples described in Section 5 and are subtracted from the measured distributions. The dominant background, $\mathrm{t\bar{t}}$, is also measured from data. This $\mathrm{t\bar{t}}$ background contributes mainly due to events with two same-flavour leptons. The production cross sections for $\mathrm{e^+e^-}$ and $\mu^+\mu^-$ events from $\mathrm{t\bar{t}}$ are identical to the cross section of $\mathrm{e}^+\mu^-$ and $\mathrm{e}^-\mu^+$ and can therefore be estimated from the latter. We select events in the $\mathrm{t\bar{t}}$ control sample using the same criteria as for the measurement, but requiring the two leptons to have different flavours. This requirement rejects the signal and provides a sample enriched in $\mathrm{t\bar{t}}$ events. Each of the distributions that we are measuring is derived from this sample and compared with the simulation. This comparison produces a discrepancy for events with at least one jet that we correct by applying a correction factor $\mathcal{C}$ to the simulation depending on the event jet multiplicity. These factors, together with their uncertainties, are given in Table 2.

After applying this correction to the simulation, all the distributions considered in this measurement agree with data in the $\mathrm{t\bar{t}}$ control sample. The agreement is demonstrated with a χ^2-test. We conclude that a parametrization as a function of the jet multiplicity is sufficient to capture the dependency on the event topology. Remaining sources of uncertainties are the estimate of the lepton reconstruction and selection efficiencies and of the yield of events from processes other than $\mathrm{t\bar{t}}$ entering in the control region. This yield is estimated from the simulation. Based on the sizes of the statistical uncertainties and background contributions, both these uncertainties are negligible. Therefore, the uncertainty in the correction factor is reduced to the statistical uncertainties in the data and simulation samples.

Table 2: The correction factors ($\mathcal{C}$) applied to the simulated $\mathrm{t\bar{t}}$ sample with their uncertainties, which are derived from the statistical uncertainties in the data and simulation samples.

N_{jets}	$\mathcal{C}$
$=0$	1
$=1$	0.94 ± 0.04
$=2$	0.97 ± 0.03
$=3$	1.01 ± 0.04
$=4$	0.86 ± 0.06
$=5$	0.61 ± 0.09
$=6$	0.68 ± 0.17

The jet multiplicity distributions in data and simulation are presented in Fig. 1. The background contamination is below 1% for the inclusive cross section, and increases with the number of jets to close to 10% for a jet multiplicity of three and above due to $\mathrm{t\bar{t}}$ production. Multijet and W events could pass the selection if one or two jets are misidentified as leptons. The number of multijet events is estimated from data using a control sample obtained by requiring two same-sign same-flavour lepton candidates, whereas the number of W events is estimated from simulation. Both contributions are found to be negligible. Fig. 2 shows the $p_{\mathrm{T}}^{\mathrm{bal}}$ distribution separately for electron and muon channels. The $\mathrm{t\bar{t}}$ background does not peak at the same p_{T} balance as the signal, and has a broader spectrum. The JZB distribution is shown in Fig. 3. The $\mathrm{t\bar{t}}$ background is asymmetric, making a larger contribution to the positive side of the distribution because transverse energy is carried away by neutrinos from W boson decays, leading to a

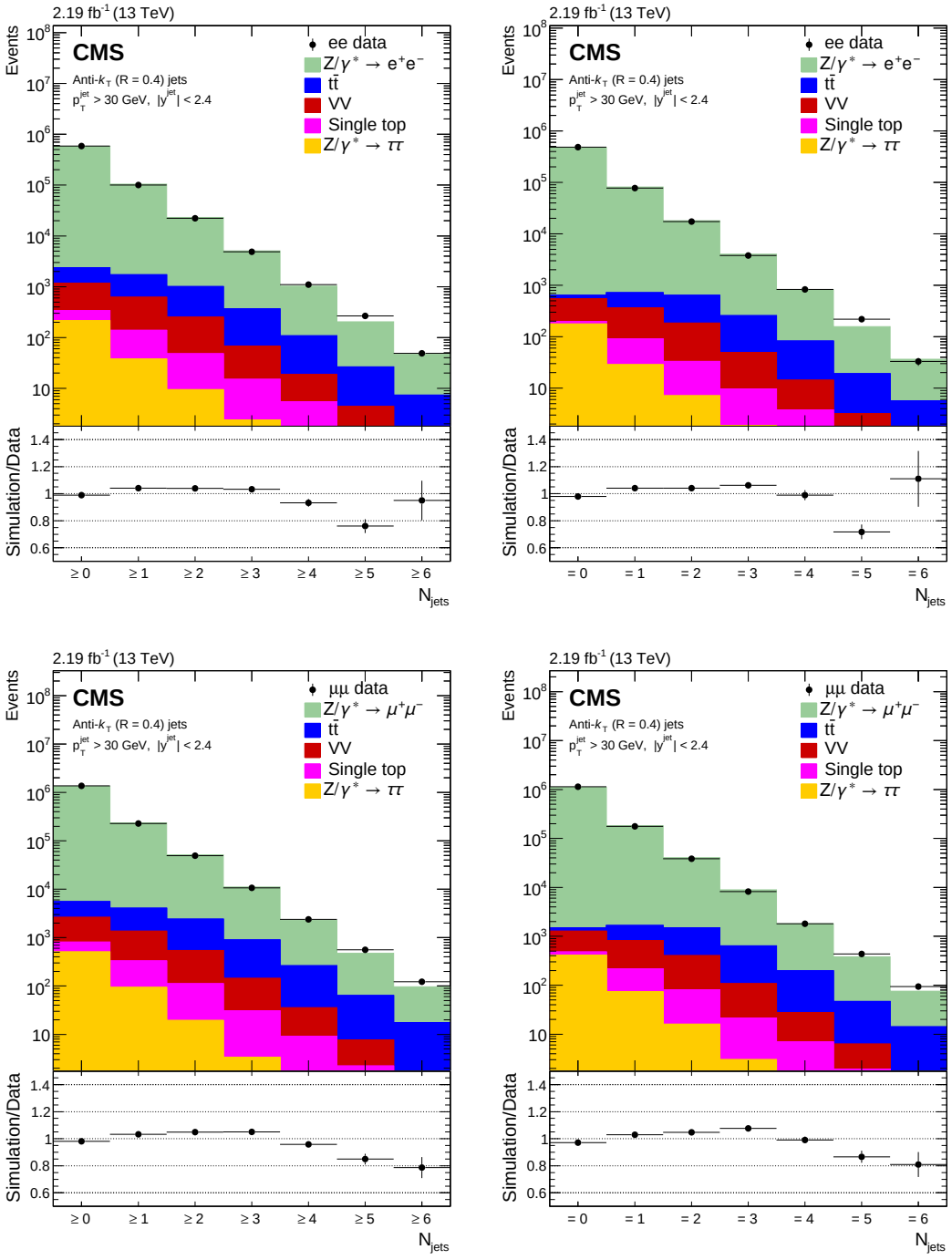

Figure 1: Reconstructed data, simulated signal, and background distributions of the inclusive (left) and exclusive (right) jet multiplicity for the electron (upper) and muon (lower) channels. The background distributions are obtained from the simulation, except for the $\mathrm{t\bar{t}}$ contribution which is estimated from the data as explained in the text. The error bars correspond to the statistical uncertainty. In the ratio plots, they include both the uncertainties from data and from simulation. The set of generators described in Section 5 has been used for the simulation.

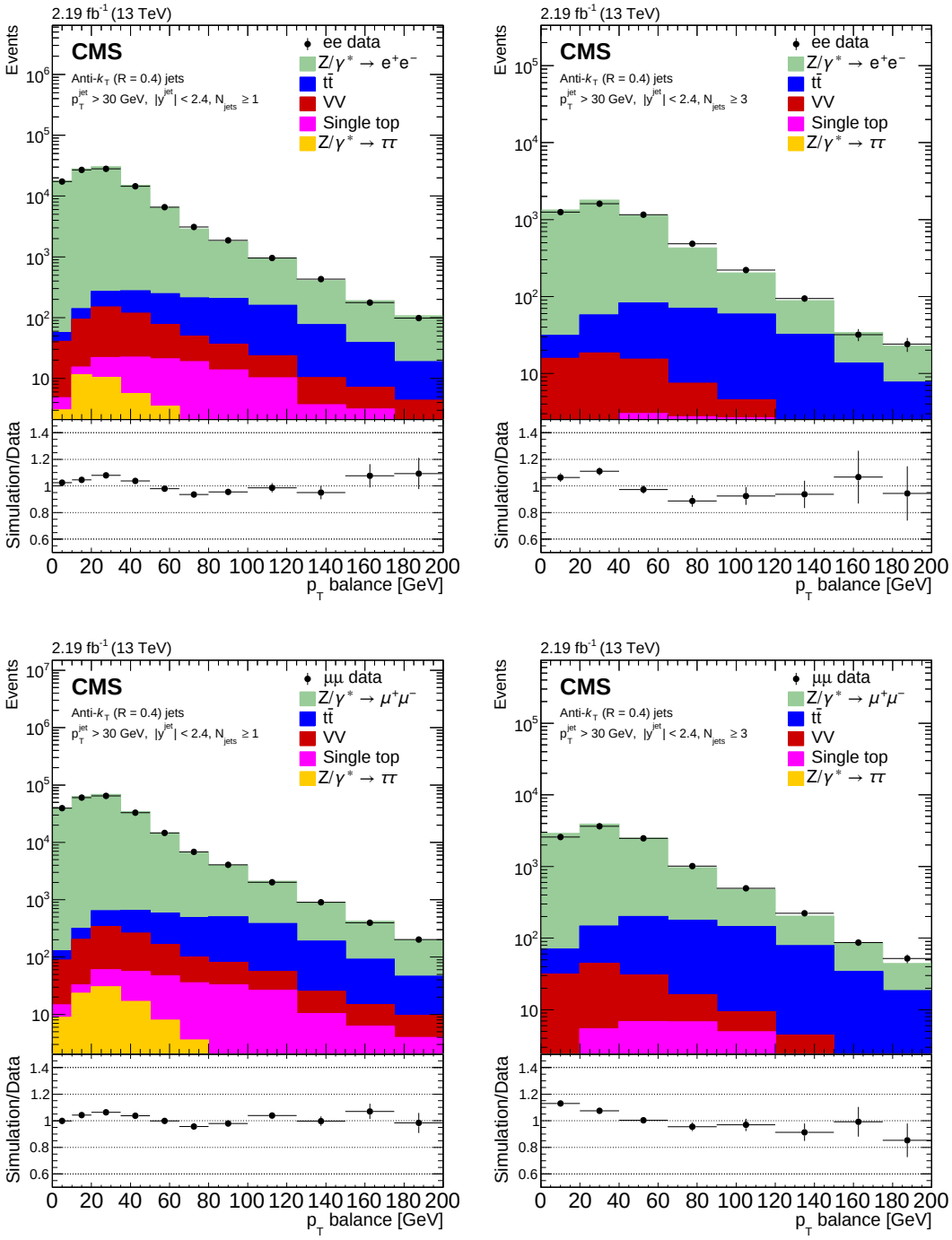

Figure 2: Reconstructed data, simulated signal, and background distributions of the transverse momentum balance between the Z boson and the sum of the jets with at least one jet (left) and three jets (right) for the electron (upper) and muon (lower) channels. The background distributions are obtained from the simulation, except for the $t\bar{t}$ contribution which is estimated from the data as explained in the text. The error bars correspond to the statistical uncertainty. In the ratio plots, they include both the uncertainties from data and from simulation. The set of generators described in Section 5 has been used for the simulation.

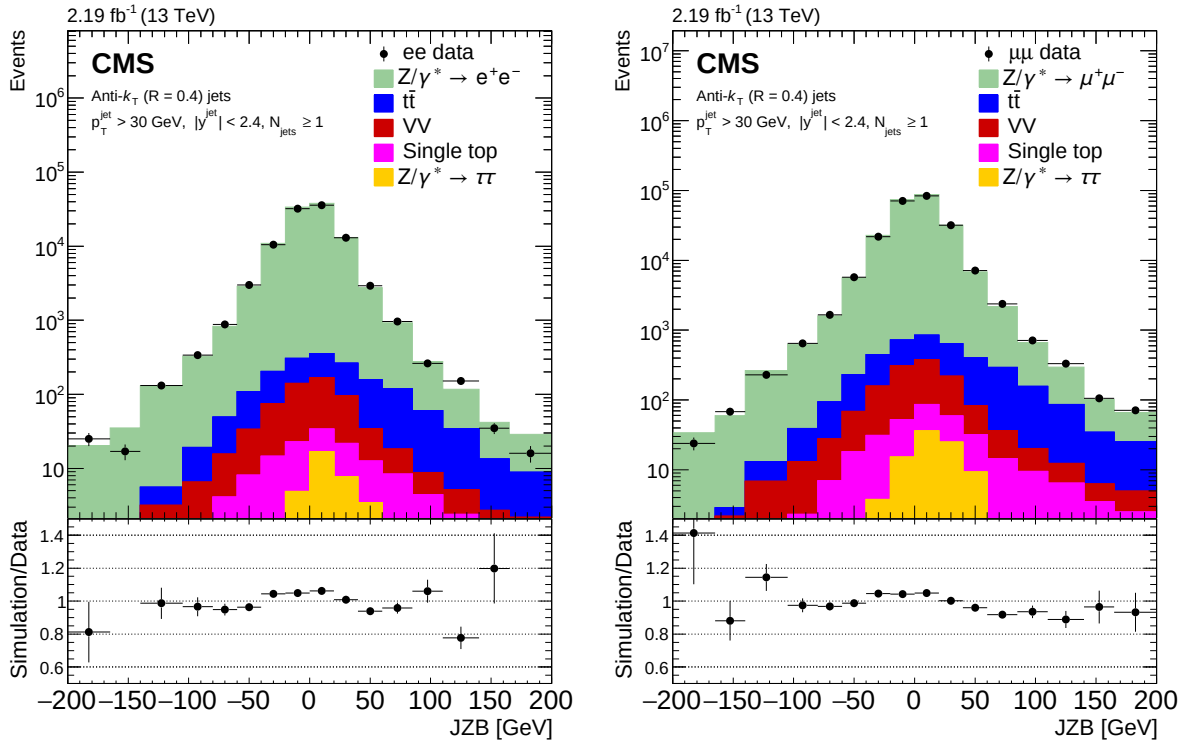

Figure 3: Reconstructed data, simulated signal, and background distributions of the JZB variable for the electron (left) and muon (right) channels. The background distributions are obtained from the simulation, except for the $t\bar{t}$ contribution which is estimated from the data as explained in the text. The error bars correspond to the statistical uncertainty. In the ratio plots, they include both the uncertainties from data and from simulation. The set of generators described in Section 5 has been used for the simulation.

reduction in the negative term of the JZB expression. Overall the agreement between data and simulation before the background subtraction is good and differences are within about 10%.

8 Unfolding procedure

The fiducial cross sections are obtained by subtracting the simulated backgrounds from the data distributions and correcting the background-subtracted data distributions back to the particle level using an unfolding procedure, which takes into account detector effects such as detection efficiency and resolution. The unfolding is performed using the D'Agostini iterative method with early stopping [51] implemented in the RooUnfold toolkit [52]. The response matrix describes the migration probability between the particle- and reconstructed-level quantities, including the overall reconstruction efficiencies. It is computed using a $\mathrm{Z}+$ jets sample simulated with MG5_aMC interfaced with PYTHIA8, using the FxFx merging scheme as described in Section 4. The optimal number of iterations is determined separately for each distribution by studying the fluctuations introduced by the unfolding with toy MC experiments generated at each step of the iteration. Final unfolded results have also been checked to be consistent with data-simulation comparisons on detector-folded distributions.

Because of the steep slope at the lower boundary of the jet transverse momentum distributions and in order to improve its accuracy, the unfolding is performed for these distributions using histograms with two additional bins, $[20, 24]$ and $[24, 30]$ GeV, below the nominal p_{T} threshold. The additional bins are discarded after the unfolding

The particle-level values refer to the stable leptons from the decay of the Z boson and to the jets built from the stable particles ($c\tau > 1$ cm) other than neutrinos using the same algorithm as for the measurements. The momenta of all the photons whose R distance to the lepton axis is smaller than 0.1 are added to the lepton momentum to account for the effects of the final-state radiation; the leptons are said to be "dressed". The momentum of the Z boson is taken to be the sum of the momenta of the two highest-p_{T} electrons (or muons). The phase space for the cross section measurement is restricted to events with a Z boson mass between 71 and 111 GeV and both leptons with $p_{\mathrm{T}} > 20$ GeV and $|\eta| < 2.4$. Jets are required to have $p_{\mathrm{T}} > 30$ GeV, $|y| < 2.4$ and a spatial separation from the dressed leptons of $R > 0.4$.

9 Systematic uncertainties

The systematic uncertainties are propagated to the measurement by varying the corresponding simulation parameters by one standard deviation up and down when computing the response matrix. The uncertainty sources are independent, and the resulting uncertainties are therefore added in quadrature. Tables 3 to 20 present the uncertainties for each differential cross section.

The dominant uncertainty comes from the jet energy scale (JES). It typically amounts to 5% for a jet multiplicity of one and increases with the number of reconstructed jets. The uncertainty in the jet resolution (JER), which is responsible for the bin-to-bin migrations that is corrected by the unfolding, is estimated and the resulting uncertainty is typically 1%.

The most important uncertainty after the JES arises from the measured efficiency (Eff) of trigger, lepton reconstruction, and lepton identification, which results in a measurement uncertainty of about 2% up to 4% for events with leptons of large transverse momenta. The uncertainty in the measurement of the integrated luminosity (Lumi) is 2.3% [53]. The resulting uncertainty on the measured distributions is 2.3%, although the uncertainty is slightly larger in regions that contain background contributions that are estimated from simulation.

Table 3: Cross section in exclusive jet multiplicity for the combination of both decay channels and breakdown of the uncertainties.

N_{jets}	$\frac{d\sigma}{dN_{\text{jets}}}$ [pb]	Tot. unc [%]	Stat [%]	JES [%]	JER [%]	Eff [%]	Lumi [%]	Bkg [%]	Pileup [%]	Unf model [%]	Unf stat [%]
$= 0$	652.	3.0	0.090	1.1	0.046	1.5	2.3	<0.01	0.22	—	0.026
$= 1$	98.0	5.1	0.27	4.3	0.18	1.5	2.3	0.012	0.30	—	0.10
$= 2$	22.3	7.3	0.62	6.7	0.20	1.6	2.3	0.026	0.43	—	0.26
$= 3$	4.68	10.	1.3	9.8	0.39	1.7	2.3	0.13	0.29	—	0.54
$= 4$	1.01	11.	3.4	10.	0.24	1.7	2.3	0.42	0.56	—	1.4
$= 5$	0.274	14.	5.0	12.	0.076	2.0	2.3	1.2	0.30	—	2.2
$= 6$	0.045	24.	15.	17.	0.35	1.8	2.4	3.5	1.7	—	6.6

Table 4: Cross section in inclusive jet multiplicity for the combination of both decay channels and breakdown of the uncertainties.

N_{jets}	$\frac{d\sigma}{dN_{\text{jets}}}$ [pb]	Tot. unc [%]	Stat [%]	JES [%]	JER [%]	Eff [%]	Lumi [%]	Bkg [%]	Pileup [%]	Unf model [%]	Unf stat [%]
≥ 0	778.	2.8	0.080	0.079	<0.01	1.5	2.3	<0.01	0.24	—	0.025
≥ 1	126.3	5.7	0.22	5.0	0.19	1.5	2.3	<0.01	0.32	—	0.086
≥ 2	28.3	7.9	0.51	7.4	0.22	1.6	2.3	0.072	0.41	—	0.21
≥ 3	6.02	11.	1.1	10.	0.29	1.7	2.3	0.25	0.35	—	0.46
≥ 4	1.33	12.	2.7	11.	0.16	1.7	2.3	0.65	0.54	—	1.1
≥ 5	0.319	14.	4.8	13.	0.097	1.9	2.3	1.5	0.50	—	2.2
≥ 6	0.045	24.	15.	17.	0.35	1.8	2.4	3.5	1.7	—	6.6

The largest background contribution to the uncertainty (Bkg) comes from the reweighting procedure for the $\bar{t}t$ simulation, which is estimated to be less than 1% for jet multiplicity below 4. Theoretical contributions come from the accuracy of the predicted cross sections, and include the uncertainties from PDFs, α_S and the fixed-order calculation. Three other small sources of uncertainty are: (1) the lepton energy scale (LES) and resolution (LER), which are below 0.3% in every bin of the measured distributions; (2) the uncertainty in the pileup model, where the 5% uncertainty in the average number of pileup events results in an uncertainty in the measurement smaller than 1%; and (3) the uncertainty in the input distribution used to build the response matrix used in the unfolding and described as follows.

Because of the finite binning a different distribution will lead to a different response matrix. This uncertainty is estimated by weighting the simulation to agree with the data in each distribution and building a new response matrix. The weighting is done using a finer binning than for the measurement. The difference between the nominal results and the results unfolded using the alternative response matrix is taken as the systematic uncertainty, denoted *Unf model*. An additional uncertainty comes from the finite size of the simulation sample used to build the response matrix. This source of uncertainty is denoted *Unf stat* in the table and is included in the systematic uncertainty of the measurement.

10 Results

The measurements from the electron and muon channels are found to be consistent and are combined using a weighted average as described in Ref. [6]. For each bin of the measured differential cross sections, the results of each of the two measurements are weighted by the inverse of the squared total uncertainty. The covariance matrix of the combination, the diagonal elements of which are used to extract the measurement uncertainties, is computed assuming full correlation between the two channels for all the sources of uncertainty sources except the statistical uncertainties and those associated with lepton reconstruction and identification, which

Table 5: Differential cross section in $p_T(Z)$ ($N_{jets} \geq 1$) for the combination of both decay channels and breakdown of the uncertainties.

$p_T(Z)$	$\frac{d\sigma}{dp_T(Z)}$	Tot. unc	Stat	JES	JER	Eff	Lumi	Bkg	LES	LER	Pileup	Unf model	Unf stat
[GeV]	$[\frac{pb}{GeV}]$	[%]	[%]	[%]	[%]	[%]	[%]	[%]	[%]	[%]	[%]	[%]	[%]
0...1.25	0.073	18.	5.4	16.	0.81	1.6	2.3	<0.01	1.2	0.93	0.22	5.5	2.2
1.25...2.5	0.212	14.	3.2	13.	0.89	1.6	2.3	<0.01	0.67	0.37	0.34	1.9	1.3
2.5...3.75	0.309	13.	2.7	13.	0.82	1.5	2.3	<0.01	0.55	0.30	0.17	1.7	1.1
3.75...5	0.377	13.	2.4	13.	0.86	1.6	2.3	<0.01	0.73	0.18	0.43	1.2	1.0
5...6.25	0.422	14.	2.3	13.	0.85	1.5	2.3	<0.01	0.55	0.085	0.50	1.7	1.1
6.25...7.5	0.487	13.	2.2	12.	0.88	1.5	2.3	<0.01	0.51	0.11	0.34	1.8	1.0
7.5...8.75	0.537	13.	2.1	12.	0.85	1.5	2.3	<0.01	0.57	0.073	0.30	2.0	1.0
8.75...10	0.580	12.	1.9	12.	0.81	1.6	2.3	<0.01	0.62	0.040	0.24	2.7	0.93
10...11.25	0.631	13.	1.9	12.	0.74	1.6	2.3	<0.01	0.67	0.030	0.29	3.1	0.91
11.25...12.5	0.697	12.	1.8	11.	0.81	1.6	2.3	<0.01	0.55	0.11	0.20	3.2	0.91
12.5...15	0.757	12.	1.4	11.	0.89	1.6	2.3	<0.01	0.48	0.098	0.18	2.8	0.71
15...17.5	0.87	12.	1.4	11.	0.86	1.5	2.3	<0.01	0.98	0.093	0.058	2.2	0.68
17.5...20	0.98	12.	1.3	12.	0.87	1.5	2.3	<0.01	0.81	0.085	0.43	1.1	0.66
20...25	1.15	11.	0.87	11.	0.79	1.6	2.3	<0.01	0.67	0.044	0.19	1.4	0.43
25...30	1.47	11.	0.79	10.	0.54	1.6	2.3	<0.01	0.63	0.017	0.30	1.4	0.36
30...35	1.80	9.3	0.75	8.6	0.32	1.5	2.3	<0.01	0.50	0.035	0.45	1.9	0.32
35...40	2.03	7.3	0.69	6.4	0.11	1.6	2.3	<0.01	0.26	0.055	0.35	1.7	0.28
40...45	2.04	6.0	0.72	5.0	0.061	1.6	2.3	<0.01	0.11	0.046	0.38	1.5	0.29
45...50	1.908	4.9	0.74	3.8	0.028	1.6	2.3	<0.01	0.18	0.034	0.39	1.0	0.29
50...60	1.617	3.9	0.59	2.5	0.025	1.5	2.3	0.012	0.22	0.039	0.41	0.74	0.23
60...70	1.204	3.4	0.68	1.6	0.023	1.6	2.3	0.018	0.51	0.031	0.23	0.53	0.26
70...80	0.881	3.2	0.77	1.0	0.017	1.6	2.3	0.024	0.65	0.055	0.38	0.52	0.30
80...90	0.634	3.3	0.87	0.64	0.011	1.6	2.3	0.028	0.93	<0.01	0.25	0.63	0.35
90...100	0.444	3.3	1.0	0.38	0.022	1.6	2.3	0.031	0.80	0.081	0.36	0.74	0.42
100...110	0.333	3.3	1.2	0.34	<0.01	1.6	2.3	0.026	0.66	<0.01	0.25	0.77	0.48
110...130	0.2212	3.3	1.0	0.22	<0.01	1.6	2.3	0.021	0.87	0.019	0.20	0.79	0.41
130...150	0.1308	3.4	1.3	0.16	0.010	1.7	2.3	0.021	0.88	0.023	0.073	0.88	0.54
150...170	0.0813	3.6	1.6	0.18	0.013	1.7	2.3	0.016	0.75	0.027	0.11	1.0	0.67
170...190	0.0516	3.9	2.0	0.13	0.015	1.8	2.3	0.022	0.87	0.017	0.17	1.1	0.84
190...220	0.0317	4.0	2.1	0.11	<0.01	1.8	2.3	0.034	0.69	0.033	0.10	1.1	0.90
220...250	0.01835	4.5	2.8	0.028	<0.01	1.8	2.3	0.041	0.82	0.020	0.11	1.4	1.2
250...400	0.00508	4.5	2.5	0.055	<0.01	2.0	2.3	0.065	0.80	<0.01	0.12	1.4	1.1
400...1000	0.000187	7.8	6.1	<0.01	<0.01	1.7	2.4	0.11	1.7	0.062	0.58	2.6	2.4

Table 6: Differential cross section in 1st jet p_T ($N_{jets} \geq 1$) for the combination of both decay channels and breakdown of the uncertainties.

$p_T(j_1)$	$\frac{d\sigma}{dp_T(j_1)}$	Tot. unc	Stat	JES	JER	Eff	Lumi	Bkg	Pileup	Unf model	Unf stat
[GeV]	$[\frac{pb}{GeV}]$	[%]	[%]	[%]	[%]	[%]	[%]	[%]	[%]	[%]	[%]
30...41	3.99	5.9	0.28	5.1	0.17	1.5	2.3	<0.01	0.39	0.34	0.11
41...59	2.07	5.4	0.35	4.5	0.18	1.5	2.3	0.011	0.33	0.35	0.13
59...83	0.933	5.1	0.45	4.2	0.17	1.6	2.3	0.015	0.25	0.26	0.18
83...118	0.377	5.1	0.59	4.1	0.20	1.6	2.3	0.051	0.28	0.24	0.24
118...168	0.1300	5.1	0.92	4.1	0.22	1.6	2.3	0.070	0.057	0.30	0.38
168...220	0.0448	4.9	1.4	3.8	0.21	1.6	2.3	0.077	0.21	0.30	0.59
220...300	0.01477	6.4	2.0	5.3	0.32	1.6	2.3	0.065	0.30	0.37	0.86
300...400	0.00390	7.0	3.4	5.2	0.24	1.7	2.3	0.096	0.28	0.72	1.4

Table 7: Differential cross section in 2nd jet p_T ($N_{jets} \geq 2$) for the combination of both decay channels and breakdown of the uncertainties.

$p_T(j_2)$ [GeV]	$\frac{d\sigma}{dp_T(j_2)}$ [$\frac{pb}{GeV}$]	Tot. unc [%]	Stat [%]	JES [%]	JER [%]	Eff [%]	Lumi [%]	Bkg [%]	Pileup [%]	Unf model [%]	Unf stat [%]
30...41	1.125	8.5	0.56	7.9	0.22	1.6	2.3	0.020	0.51	0.38	0.24
41...59	0.457	7.4	0.73	6.8	0.13	1.6	2.3	0.049	0.33	0.34	0.31
59...83	0.173	6.5	1.1	5.7	0.16	1.6	2.3	0.15	0.31	0.39	0.44
83...118	0.0590	5.6	1.7	4.4	0.16	1.6	2.3	0.22	0.48	0.21	0.66
118...168	0.0187	6.0	2.3	4.7	0.20	1.7	2.3	0.25	0.19	0.13	0.89
168...250	0.00518	6.6	3.4	4.6	0.33	1.7	2.3	0.22	0.21	0.19	1.3

Table 8: Differential cross section in 3rd jet p_T ($N_{jets} \geq 3$) for the combination of both decay channels and breakdown of the uncertainties.

$p_T(j_3)$ [GeV]	$\frac{d\sigma}{dp_T(j_3)}$ [$\frac{pb}{GeV}$]	Tot. unc [%]	Stat [%]	JES [%]	JER [%]	Eff [%]	Lumi [%]	Bkg [%]	Pileup [%]	Unf model [%]	Unf stat [%]
30...41	0.289	11.	1.2	10.	0.26	1.6	2.3	0.12	0.42	0.93	0.50
41...59	0.0972	9.3	1.8	8.6	0.14	1.7	2.3	0.28	0.41	1.0	0.72
59...83	0.0306	7.9	2.9	6.5	0.31	1.7	2.3	0.48	0.69	1.2	1.1
83...118	0.00756	11.	4.7	8.7	0.46	1.9	2.3	0.83	0.74	0.83	1.7
118...168	0.00180	10.	8.1	3.7	0.40	1.8	2.4	0.82	0.50	1.3	3.0
168...250	0.000342	17.	14.	6.1	0.20	1.8	2.3	0.71	1.5	2.2	5.3

Table 9: Differential cross section in 1st jet $|y|$ ($N_{jets} \geq 1$) for the combination of both decay channels and breakdown of the uncertainties.

$\lvert y(j_1)\rvert$	$\frac{d\sigma}{d\lvert y(j_1)\rvert}$ [pb]	Tot. unc [%]	Stat [%]	JES [%]	JER [%]	Eff [%]	Lumi [%]	Bkg [%]	Pileup [%]	Unf model [%]	Unf stat [%]
0...0.2	70.4	4.9	0.62	4.0	0.089	1.5	2.3	0.015	0.23	0.11	0.25
0.2...0.4	69.5	5.0	0.63	4.1	0.097	1.5	2.3	0.015	0.29	0.14	0.26
0.4...0.6	66.7	5.0	0.65	4.1	0.12	1.5	2.3	0.014	0.20	0.14	0.26
0.6...0.8	64.7	5.2	0.64	4.3	0.18	1.6	2.3	0.014	0.30	0.15	0.26
0.8...1	62.3	5.2	0.68	4.3	0.087	1.5	2.3	0.013	0.20	0.17	0.28
1...1.2	57.3	5.1	0.71	4.2	0.19	1.5	2.3	0.012	0.28	0.24	0.29
1.2...1.4	52.0	5.4	0.75	4.6	0.16	1.5	2.3	<0.01	0.29	0.25	0.31
1.4...1.6	47.8	6.1	0.77	5.4	0.087	1.5	2.3	<0.01	0.32	0.31	0.32
1.6...1.8	43.5	6.3	0.80	5.6	0.21	1.5	2.3	<0.01	0.34	0.21	0.34
1.8...2	38.9	6.7	0.84	6.0	0.38	1.5	2.3	<0.01	0.41	0.32	0.36
2...2.2	34.3	7.2	0.90	6.5	0.44	1.5	2.3	<0.01	0.62	0.40	0.39
2.2...2.4	29.5	7.2	1.0	6.4	0.66	1.5	2.3	<0.01	0.66	0.36	0.44

Table 10: Differential cross section in 2nd jet $|y|$ ($N_{\text{jets}} \geq 2$) for the combination of both decay channels and breakdown of the uncertainties.

$\lvert y(j_2)\rvert$	$\frac{\mathrm{d}\sigma}{\mathrm{d}\lvert y(j_2)\rvert}$ [pb]	Tot. unc [%]	Stat [%]	JES [%]	JER [%]	Eff [%]	Lumi [%]	Bkg [%]	Pileup [%]	Unf model [%]	Unf stat [%]
0 ... 0.2	15.1	7.2	1.4	6.4	0.11	1.6	2.3	0.078	0.30	0.26	0.62
0.2 ... 0.4	14.4	7.3	1.5	6.6	0.041	1.6	2.3	0.082	0.15	0.33	0.64
0.4 ... 0.6	14.4	7.4	1.4	6.6	0.13	1.6	2.3	0.074	0.49	0.35	0.64
0.6 ... 0.8	13.7	7.5	1.5	6.7	0.25	1.6	2.3	0.071	0.35	0.27	0.68
0.8 ... 1	13.9	7.5	1.5	6.7	0.17	1.6	2.3	0.065	0.17	0.093	0.70
1 ... 1.2	12.43	7.4	1.6	6.6	0.11	1.6	2.3	0.065	0.42	0.13	0.70
1.2 ... 1.4	11.89	8.1	1.5	7.4	0.082	1.6	2.3	0.062	0.23	0.10	0.68
1.4 ... 1.6	11.00	7.7	1.7	6.9	0.15	1.6	2.3	0.052	0.51	0.11	0.76
1.6 ... 1.8	10.09	8.6	1.7	7.8	0.25	1.6	2.3	0.049	0.48	0.19	0.78
1.8 ... 2	9.35	8.2	1.8	7.4	0.33	1.6	2.3	0.043	0.65	0.44	0.84
2 ... 2.2	8.48	8.6	1.8	7.8	0.48	1.6	2.3	0.035	0.50	0.67	0.85
2.2 ... 2.4	7.04	9.3	2.0	8.4	0.37	1.6	2.3	0.037	0.93	1.2	0.96

Table 11: Differential cross section in 3rd jet $|y|$ ($N_{\text{jets}} \geq 3$) for the combination of both decay channels and breakdown of the uncertainties.

$\lvert y(j_3)\rvert$	$\frac{\mathrm{d}\sigma}{\mathrm{d}\lvert y(j_3)\rvert}$ [pb]	Tot. unc [%]	Stat [%]	JES [%]	JER [%]	Eff [%]	Lumi [%]	Bkg [%]	Pileup [%]	Unf model [%]	Unf stat [%]
0 ... 0.3	3.14	9.9	2.5	9.0	0.26	1.7	2.3	0.27	0.28	0.15	1.1
0.3 ... 0.6	3.02	10.	2.6	9.4	0.13	1.7	2.3	0.27	0.31	0.088	1.1
0.6 ... 0.9	3.06	9.6	2.6	8.7	0.20	1.6	2.3	0.25	0.20	0.012	1.2
0.9 ... 1.2	2.70	9.5	2.7	8.5	0.22	1.7	2.3	0.25	0.22	0.34	1.2
1.2 ... 1.5	2.51	12.	2.8	11.	0.14	1.6	2.3	0.23	0.59	0.78	1.3
1.5 ... 1.8	2.21	11.	3.1	10.	0.17	1.6	2.3	0.22	0.13	0.62	1.4
1.8 ... 2.1	1.89	13.	3.1	12.	0.13	1.7	2.3	0.22	0.57	1.8	1.4
2.1 ... 2.4	1.70	11.	3.4	10.	0.66	1.7	2.3	0.21	0.87	2.4	1.6

Table 12: Differential cross section in H_{T} ($N_{\text{jets}} \geq 1$) for the combination of both decay channels and breakdown of the uncertainties.

H_{T} [GeV]	$\frac{\mathrm{d}\sigma}{\mathrm{d}H_{\text{T}}}$ $[\frac{\text{pb}}{\text{GeV}}]$	Tot. unc [%]	Stat [%]	JES [%]	JER [%]	Eff [%]	Lumi [%]	Bkg [%]	Pileup [%]	Unf model [%]	Unf stat [%]
30 ... 41	3.71	5.9	0.41	5.1	0.18	1.5	2.3	<0.01	0.38	0.92	0.19
41 ... 59	1.678	4.7	0.53	3.6	0.16	1.5	2.3	<0.01	0.26	1.1	0.21
59 ... 83	0.852	5.3	0.66	4.4	0.23	1.5	2.3	<0.01	0.30	0.62	0.26
83 ... 118	0.449	6.0	0.74	5.3	0.13	1.6	2.3	0.015	0.34	0.54	0.30
118 ... 168	0.199	5.9	0.92	5.1	0.20	1.6	2.3	0.040	0.18	0.41	0.38
168 ... 220	0.0886	6.3	1.5	5.4	0.36	1.6	2.3	0.078	0.35	0.33	0.61
220 ... 300	0.0373	6.9	1.6	6.0	0.10	1.7	2.3	0.14	0.20	0.17	0.66
300 ... 400	0.0148	6.8	2.3	5.6	0.21	1.6	2.3	0.20	0.18	0.21	0.98
400 ... 550	0.00449	7.3	3.2	5.7	0.20	1.8	2.3	0.36	0.63	0.28	1.3
550 ... 780	0.00133	8.1	5.3	4.8	0.13	1.6	2.3	0.40	1.2	0.24	2.1
780 ... 1100	0.000306	12.	8.2	7.5	0.22	1.8	2.3	0.59	0.69	0.56	3.2

Table 13: Differential cross section in H_T ($N_{jets} \geq 2$) for the combination of both decay channels and breakdown of the uncertainties.

H_T [GeV]	$\frac{d\sigma}{dH_T}$ [$\frac{pb}{GeV}$]	Tot. unc [%]	Stat [%]	JES [%]	JER [%]	Eff [%]	Lumi [%]	Bkg [%]	Pileup [%]	Unf model [%]	Unf stat [%]
60 ... 83	0.208	9.5	1.1	8.9	0.25	1.5	2.3	0.023	0.63	1.0	0.67
83 ... 118	0.228	7.9	0.89	7.3	0.15	1.6	2.3	0.027	0.45	0.59	0.42
118 ... 168	0.1371	6.8	0.96	6.0	0.18	1.6	2.3	0.030	0.32	0.58	0.42
168 ... 220	0.0705	7.3	1.4	6.6	0.29	1.6	2.3	0.10	0.36	0.31	0.57
220 ... 300	0.0329	7.1	1.6	6.2	0.11	1.7	2.3	0.16	0.18	0.29	0.64
300 ... 400	0.01360	6.8	2.2	5.7	0.20	1.6	2.3	0.22	0.33	0.29	0.90
400 ... 550	0.00436	7.3	3.1	5.8	0.18	1.8	2.3	0.36	0.56	0.28	1.2
550 ... 780	0.00129	8.1	5.0	5.1	0.17	1.6	2.3	0.41	1.1	0.21	1.9
780 ... 1100	0.000304	12.	7.9	7.2	0.25	1.7	2.3	0.58	0.65	0.41	3.1

Table 14: Differential cross section in H_T ($N_{jets} \geq 3$) for the combination of both decay channels and breakdown of the uncertainties.

H_T [GeV]	$\frac{d\sigma}{dH_T}$ [$\frac{pb}{GeV}$]	Tot. unc [%]	Stat [%]	JES [%]	JER [%]	Eff [%]	Lumi [%]	Bkg [%]	Pileup [%]	Unf model [%]	Unf stat [%]
90 ... 130	0.0166	17.	3.5	15.	0.64	1.6	2.3	0.013	0.61	5.4	2.3
130 ... 168	0.0300	12.	2.5	11.	0.10	1.7	2.3	0.097	0.35	1.8	1.2
168 ... 220	0.0254	11.	2.8	9.7	0.088	1.7	2.3	0.20	0.46	0.75	1.2
220 ... 300	0.0163	9.3	2.4	8.4	0.27	1.7	2.3	0.28	0.21	0.73	1.0
300 ... 400	0.00841	8.4	3.1	7.2	0.13	1.7	2.3	0.36	0.26	0.43	1.3
400 ... 550	0.00307	8.9	3.9	7.2	0.22	1.8	2.3	0.53	0.72	0.40	1.5
550 ... 780	0.00103	10.	6.3	6.8	0.33	1.7	2.3	0.53	1.1	0.22	2.5
780 ... 1100	0.000246	12.	9.1	6.5	0.17	1.7	2.3	0.67	0.88	2.7	3.5

Table 15: Differential cross section in p_T^{bal} ($N_{jets} \geq 1$) for the combination of both decay channels and breakdown of the uncertainties.

p_T^{bal} [GeV]	$\frac{d\sigma}{dp_T^{bal}}$ [$\frac{pb}{GeV}$]	Tot. unc [%]	Stat [%]	JES [%]	JER [%]	Eff [%]	Lumi [%]	Bkg [%]	Pileup [%]	Unf model [%]	Unf stat [%]
0 ... 10	2.65	6.0	0.45	5.2	0.42	1.5	2.3	<0.01	0.45	1.1	0.18
10 ... 20	3.53	6.1	0.36	5.3	0.28	1.5	2.3	<0.01	0.40	1.2	0.14
20 ... 35	2.35	6.3	0.37	5.1	0.38	1.6	2.3	<0.01	0.31	2.2	0.15
35 ... 50	1.116	6.0	0.53	4.1	0.69	1.6	2.3	0.023	0.30	3.2	0.23
50 ... 65	0.467	4.4	0.87	2.2	0.77	1.6	2.3	0.053	0.092	2.0	0.39
65 ... 80	0.208	5.0	1.2	1.0	0.85	1.9	2.3	0.17	0.33	3.5	0.54
80 ... 100	0.0883	5.1	1.8	1.6	0.81	2.0	2.4	0.37	0.62	2.9	0.75
100 ... 125	0.0344	6.9	2.7	2.9	0.66	2.2	2.4	0.62	0.42	4.2	1.1
125 ... 150	0.0154	7.5	4.1	4.3	0.57	2.1	2.4	0.69	0.54	2.6	1.6
150 ... 175	0.00686	12.	6.1	7.7	0.23	2.2	2.4	0.76	0.67	4.5	2.3
175 ... 200	0.00357	12.	8.0	5.2	0.82	2.3	2.5	0.71	0.51	4.7	2.9

Table 16: Differential cross section in $p_{\mathrm{T}}^{\mathrm{bal}}$ ($N_{\mathrm{jets}} \geq 2$) for the combination of both decay channels and breakdown of the uncertainties.

$p_{\mathrm{T}}^{\mathrm{bal}}$	$\frac{\mathrm{d}\sigma}{\mathrm{d}p_{\mathrm{T}}^{\mathrm{bal}}}$	Tot. unc	Stat	JES	JER	Eff	Lumi	Bkg	Pileup	Unf model	Unf stat
[GeV]	$[\frac{\mathrm{pb}}{\mathrm{GeV}}]$	[%]	[%]	[%]	[%]	[%]	[%]	[%]	[%]	[%]	[%]
0...15	0.522	8.7	0.70	8.2	0.38	1.5	2.3	0.027	0.56	0.40	0.32
15...30	0.635	8.1	0.56	7.5	0.29	1.6	2.3	0.023	0.48	0.97	0.26
30...45	0.372	6.6	0.75	5.7	0.48	1.6	2.3	0.040	0.38	1.4	0.35
45...60	0.178	6.3	1.0	5.4	0.94	1.6	2.3	0.14	0.24	0.87	0.47
60...80	0.0738	6.7	1.4	5.0	1.2	1.9	2.3	0.35	0.29	2.6	0.60
80...100	0.0308	7.3	2.3	5.2	1.3	2.2	2.4	0.75	0.34	2.7	0.91
100...125	0.0133	8.7	3.7	5.4	1.3	2.2	2.4	1.1	0.60	4.0	1.4
125...150	0.00682	12.	5.1	9.0	0.98	2.5	2.4	1.3	0.59	4.1	1.9
150...175	0.00352	14.	7.3	10.	0.15	2.6	2.4	1.4	0.22	5.1	2.6
175...200	0.00182	15.	9.5	10.	0.33	2.3	2.5	1.2	0.78	4.3	3.0

Table 17: Differential cross section in $p_{\mathrm{T}}^{\mathrm{bal}}$ ($N_{\mathrm{jets}} \geq 3$) for the combination of both decay channels and breakdown of the uncertainties.

$p_{\mathrm{T}}^{\mathrm{bal}}$	$\frac{\mathrm{d}\sigma}{\mathrm{d}p_{\mathrm{T}}^{\mathrm{bal}}}$	Tot. unc	Stat	JES	JER	Eff	Lumi	Bkg	Pileup	Unf model	Unf stat
[GeV]	$[\frac{\mathrm{pb}}{\mathrm{GeV}}]$	[%]	[%]	[%]	[%]	[%]	[%]	[%]	[%]	[%]	[%]
0...20	0.102	12.	1.8	11.	0.71	1.5	2.3	0.044	0.57	4.4	0.78
20...40	0.106	11.	1.4	9.9	0.61	1.6	2.3	0.095	0.29	2.8	0.66
40...65	0.0483	9.3	2.2	7.8	1.2	1.7	2.3	0.33	0.32	3.0	1.0
65...90	0.0160	8.5	4.0	4.8	1.4	2.1	2.4	1.1	0.16	4.1	1.7
90...120	0.00580	13.	7.1	8.3	1.9	2.3	2.4	2.0	0.61	4.6	2.9
120...150	0.00243	23.	13.	16.	0.81	2.6	2.4	2.8	1.5	6.8	5.0
150...175	0.00127	26.	18.	16.	1.3	2.6	2.4	2.9	0.96	4.3	6.7
175...200	0.00079	26.	20.	9.9	1.8	2.8	2.5	3.1	0.41	8.5	7.4

Table 18: Differential cross section in JZB (full phase space) for the combination of both decay channels and breakdown of the uncertainties.

JZB	$\frac{\mathrm{d}\sigma}{\mathrm{dJZB}}$	Tot. unc	Stat	JES	JER	Eff	Lumi	Bkg	Pileup	Unf model	Unf stat
[GeV]	$[\frac{\mathrm{pb}}{\mathrm{GeV}}]$	[%]	[%]	[%]	[%]	[%]	[%]	[%]	[%]	[%]	[%]
$-140...-105$	0.00274	17.	11.	9.8	1.3	1.6	2.4	0.10	1.6	6.4	4.8
$-105...-80$	0.0115	11.	6.3	7.0	0.66	1.7	2.4	0.12	0.64	2.5	2.9
$-80...-60$	0.0388	15.	3.7	11.	0.73	1.7	2.4	0.061	0.82	5.7	1.7
$-60...-40$	0.153	14.	2.0	11.	0.73	1.7	2.3	0.047	0.59	7.0	0.90
$-40...-20$	0.658	9.0	0.96	6.7	1.3	1.7	2.3	0.012	0.53	4.7	0.40
$-20...0$	2.45	8.0	0.43	6.9	0.54	1.6	2.3	<0.01	0.46	2.8	0.17
0...20	2.16	5.1	0.58	3.6	0.64	2.1	2.3	<0.01	0.17	1.3	0.24
20...40	0.69	15.	0.89	14.	1.5	1.6	2.3	0.027	0.41	5.4	0.38
40...60	0.142	11.	2.1	9.5	1.4	1.7	2.3	0.18	0.34	3.9	0.92
60...85	0.0356	13.	3.9	11.	1.9	1.9	2.4	0.55	1.0	2.6	1.6
85...110	0.0114	14.	7.3	9.1	0.83	2.1	2.4	0.93	2.0	5.7	3.0
110...140	0.0053	19.	11.	12.	0.66	2.4	2.5	1.1	1.5	8.0	4.4

Table 19: Differential cross section in JZB ($p_{\mathrm{T}}(\mathrm{Z}) < 50$ GeV) for the combination of both decay channels and breakdown of the uncertainties.

JZB [GeV]	$\frac{\mathrm{d}\sigma}{\mathrm{dJZB}}$ $[\frac{\mathrm{pb}}{\mathrm{GeV}}]$	Tot. unc [%]	Stat [%]	JES [%]	JER [%]	Eff [%]	Lumi [%]	Bkg [%]	Pileup [%]	Unf model [%]	Unf stat [%]
$-50\ldots-30$	0.00859	7.8	5.8	1.9	1.2	1.8	2.3	0.042	0.92	2.5	2.6
$-30\ldots-15$	0.1212	5.1	2.1	1.5	2.6	2.3	2.3	0.042	0.19	0.61	1.0
$-15\ldots0$	1.30	8.0	0.52	6.9	0.26	1.7	2.3	<0.01	0.55	2.9	0.23
$0\ldots15$	1.63	12.	0.44	11.	0.51	1.6	2.3	<0.01	0.32	3.1	0.19
$15\ldots30$	0.83	14.	0.65	13.	1.3	1.6	2.3	0.013	0.34	3.4	0.29
$30\ldots50$	0.219	11.	1.2	11.	1.4	1.6	2.3	0.036	0.15	1.2	0.50
$50\ldots75$	0.0410	11.	2.6	9.2	1.4	1.8	2.3	0.29	0.39	4.6	1.1
$75\ldots105$	0.0097	13.	5.4	9.6	0.63	2.3	2.4	0.89	1.0	6.1	2.2
$105\ldots150$	0.00241	14.	10.	6.3	1.4	2.4	2.4	1.3	0.87	5.1	3.8

Table 20: Differential cross section in JZB ($p_{\mathrm{T}}(\mathrm{Z}) > 50$ GeV) for the combination of both decay channels and breakdown of the uncertainties.

JZB [GeV]	$\frac{\mathrm{d}\sigma}{\mathrm{dJZB}}$ $[\frac{\mathrm{pb}}{\mathrm{GeV}}]$	Tot. unc [%]	Stat [%]	JES [%]	JER [%]	Eff [%]	Lumi [%]	Bkg [%]	Pileup [%]	Unf model [%]	Unf stat [%]
$-165\ldots-125$	0.00165	11.	8.8	1.6	0.32	1.7	2.4	0.15	0.87	3.3	5.0
$-125\ldots-95$	0.00475	8.8	6.2	2.8	1.3	1.9	2.4	0.14	0.46	2.0	3.4
$-95\ldots-70$	0.0182	19.	3.6	16.	0.64	1.8	2.4	0.12	0.30	5.2	2.0
$-70\ldots-45$	0.091	14.	1.4	13.	0.36	1.6	2.3	0.052	0.58	3.5	0.78
$-45\ldots-20$	0.551	6.1	0.63	3.8	0.71	1.6	2.3	0.011	0.28	1.0	0.33
$-20\ldots0$	1.404	5.3	0.38	4.4	0.13	1.5	2.3	<0.01	0.43	0.33	0.18
$0\ldots25$	0.607	4.9	0.62	3.4	0.92	2.1	2.3	0.021	0.30	1.1	0.30
$25\ldots55$	0.090	19.	1.3	18.	2.3	1.7	2.3	0.14	0.43	3.5	0.68
$55\ldots85$	0.0162	19.	3.5	14.	2.4	2.0	2.4	0.52	0.93	11.	1.8
$85\ldots120$	0.00454	18.	6.9	14.	3.2	2.0	2.4	0.79	1.8	8.1	3.3
$120\ldots150$	0.00195	21.	11.	14.	1.2	2.3	2.6	1.3	1.8	9.4	5.0

are taken to be uncorrelated. The integrated cross section is measured for different exclusive and inclusive multiplicities and the results are shown in Tables 3 and 4.

The results for the differential cross sections are shown in Figs. 4 to 15 and are compared to the predictions described in Section 4. For the two predictions obtained from MG5_aMC and PYTHIA8 the number of partons included in the ME calculation and the order of the calculation is indicated by distinctive labels ("$\leq$4j LO" for up to four partons at LO and "$\leq$2j NLO" for up to two partons at NLO). The prediction of GENEVA is denoted as "GE". The label "PY8" indicates that PYTHIA8 is used in these calculations for the parton showering and the hadronisation. The NNLO $Z + 1$ jet calculation is denoted as N_{jetti} NNLO in the legends. The measured cross section values along with the uncertainties discussed in Section 9 are given in Tables 3 to 20.

Fig. 4 shows the measured cross section as a function of the exclusive (Table 3) and the inclusive (Table 4) jet multiplicities. Agreement between the measurement and the MG5_aMC prediction is observed. The cross section obtained from LO MG5_aMC tends to be lower than NLO MG5_aMC up to a jet multiplicity of 3. The total cross section for $Z(\rightarrow \ell^+\ell^-) + \geq 0$ jet, $m_{\ell^+\ell^-} > 50\,\text{GeV}$ computed at NNLO and used to normalise the cross section of the LO prediction is similar to the NLO cross section as seen in Table 1. The smaller cross section seen when requiring at least one jet is explained by a steeply falling p_T spectrum of the leading jet in the LO prediction. The GENEVA prediction describes the measured cross section up to a jet multiplicity of 2, but fails to describe the data for higher jet multiplicities, where one or more jets arise from the parton shower. This effect is not seen in the NLO (LO) MG5_aMC predictions, which give a fair description of the data for multiplicities above three (four).

The measured cross section as a function of the transverse momentum of the Z boson for events with at least one jet is presented in Fig. 5 and Table 5. The best model for describing the measurement at low p_T, below the peak, is NLO MG5_aMC, showing a better agreement than the NNLL$_\tau$' calculation from GENEVA. The shape of the distribution in the region below 10 GeV is better described by GENEVA than by the other predictions, as shown by the flat ratio plot. This kinematic region is covered by events with extra hadronic activity in addition to the jet required by the event selection. The estimation of the uncertainty in the shape in this region shows that it is dominated by the statistical uncertainty, represented by error bars on the plot since the systematic uncertainties are negligible. In the intermediate region, GENEVA predicts a steeper rise for the distribution than the other two predictions and than the measurement. The high-p_T region, where GENEVA and NLO MG5_aMC are expected to have similar accuracy (NLO), is equally well described by the two. The LO predictions undershoot the measurement in this region despite the normalisation of the total $Z+ \geq 0$ jet cross section to its NNLO value.

The jet transverse momenta for the 1st, 2nd and 3rd leading jets can be seen in Figs. 6 and 7 (Tables 6–8). The LO MG5_aMC predicted spectrum differs from the measurement, showing a steeper slope in the low p_T region. The same feature was observed in the previous measurements [3, 4]. The comparison with NLO MG5_aMC and N_{jetti} NNLO calculation shows that adding NLO terms cures this discrepancy. The GENEVA prediction shows good agreement for the measured p_T of the first jet, while it undershoots the data at low p_T for the second jet. The jet rapidities for the first three leading jets have also been measured and the distributions are shown in Figs. 8 and 9 (Tables 9–11). All the predictions are in agreement with data.

The total jet activity has been measured via the H_T variable. The differential cross section as a function of this observable is presented in Figs. 10 and 11 (Tables 12–14) for inclusive jet multiplicities of 1, 2, and 3. The LO MG5_aMC calculation predicts fewer events than found in the data for the region $H_T < 400\,\text{GeV}$. For higher jet multiplicities both LO and NLO MG5_aMC are compatible with the measurement, although the contribution in the region $H_T < 400\,\text{GeV}$

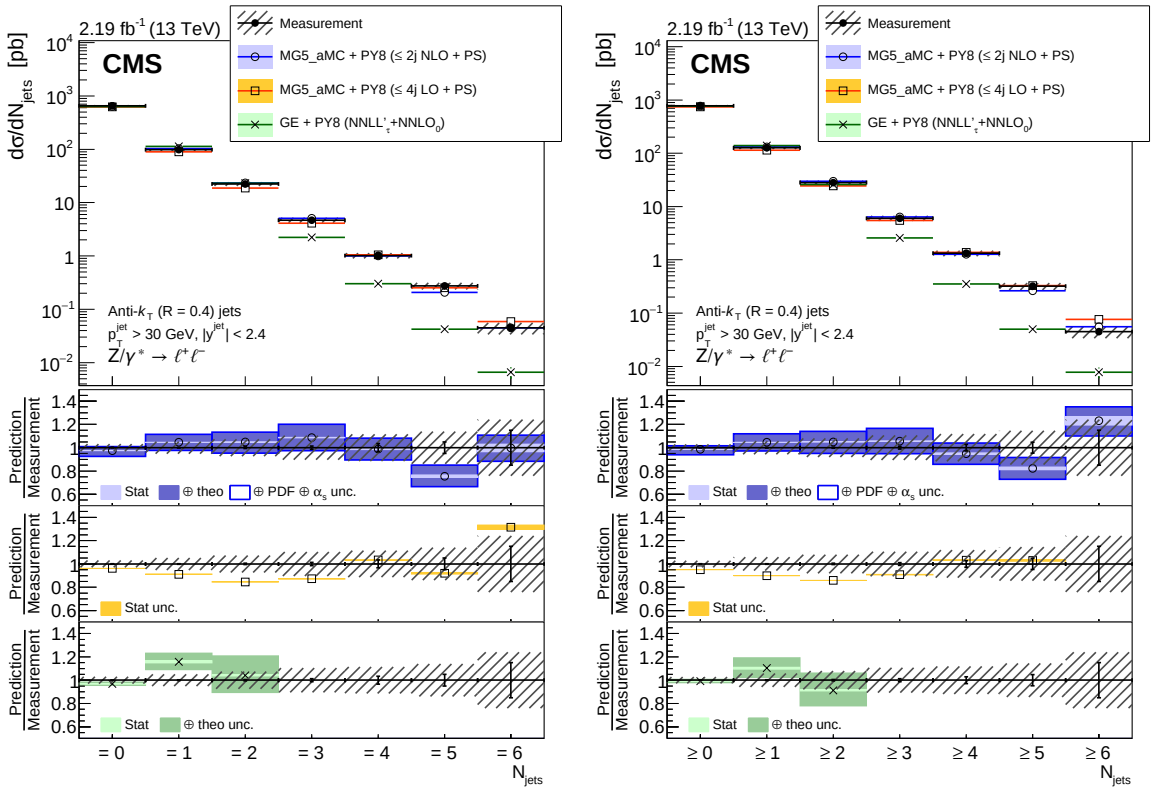

Figure 4: Measured cross section for Z + jets as a function of the jet exclusive (left) and inclusive (right) multiplicity. The error bars represent the statistical uncertainty and the grey hatched bands represent the total uncertainty, including the systematic and statistical components. The measurement is compared with different predictions, which are described in the text. The ratio of each prediction to the measurement is shown together with the measurement statistical (black bars) and total (black hatched bands) uncertainties and the prediction (coloured bands) uncertainties. Different uncertainties were considered for the predictions: statistical (stat), ME calculation (theo), and PDF together with the strong coupling constant (α_S). The complete set was computed for one of the predictions. These uncertainties were added together in quadrature (represented by the $\oplus$ sign in the legend).

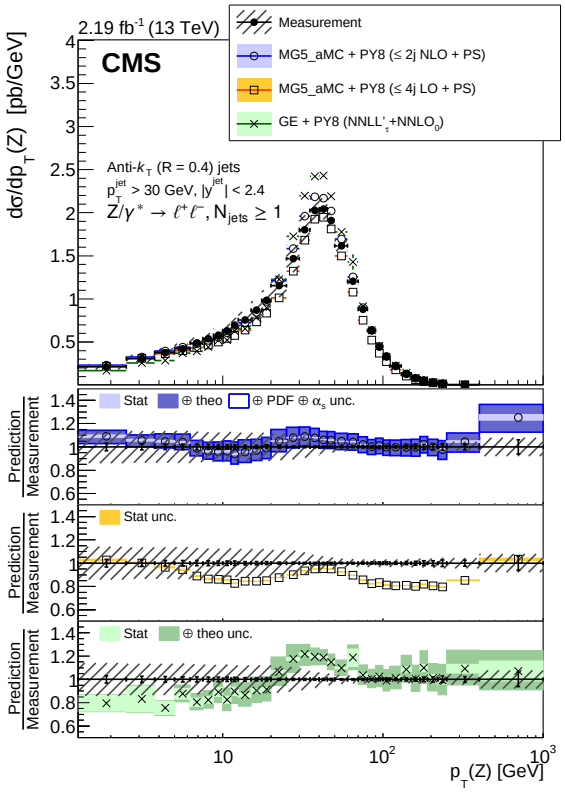

Figure 5: Measured cross section for Z + jets as a function of the transverse momentum of the Z boson for events with at least one jet. Other details are as mentioned in the Fig. 4 caption.

is smaller for LO than for NLO MG5_aMC. The contribution at lower values of H_T is slightly overestimated, but the discrepancy is compatible with the theoretical and experimental uncertainties. The GENEVA generator predicts a steeper spectrum than measured. For jet multiplicities of at least one, we also compare with N_{jetti} NNLO, and the level of agreement is similar to that found with NLO MG5_aMC. The uncertainty for N_{jetti} NNLO is larger than in the jet transverse momentum distribution because of the contribution from the additional jets.

The balance in transverse momentum between the jets and the Z boson, p_T^{bal}, is shown in Figs. 12 and 13 (Tables 15–17) for inclusive jet multiplicities of 1, 2, and 3. When more jets are included, the peak of p_T^{bal} is shifted to larger values. The measurement is in good agreement with NLO MG5_aMC predictions. The slopes of the distributions for the first two jet multiplicities predicted by LO MG5_aMC do not fully describe the data. This observation indicates that the NLO correction is important for the description of hadronic activity beyond the jet acceptance used in this analysis, $p_T > 30\,GeV$ and $|y| > 2.4$. An imbalance in the event, i.e. p_T^{bal} not equal to zero, requires two partons in the final state with one of the two out of the acceptance. Such events are described with NLO accuracy for the NLO MG5_aMC sample and LO accuracy for the two other samples. In the case of the GENEVA simulation, when at least two jets are required, as in the second plot of Fig. 12, the additional jet must come from parton showering and this leads to an underestimation of the cross section, as in the case of the jet multiplicity distribution. When requiring two jets within the acceptance, the NLO MG5_aMC prediction, which has an effective LO accuracy for this observable, starts to show discrepancies with the measurement. The estimated theoretical uncertainties cover the observed discrepancies.

The JZB distribution is shown in Figs. 14 and 15 (Tables 18–20) for the inclusive one-jet events, in the full phase space, and separately for $p_T(Z)$ below and above 50 GeV. As expected in the

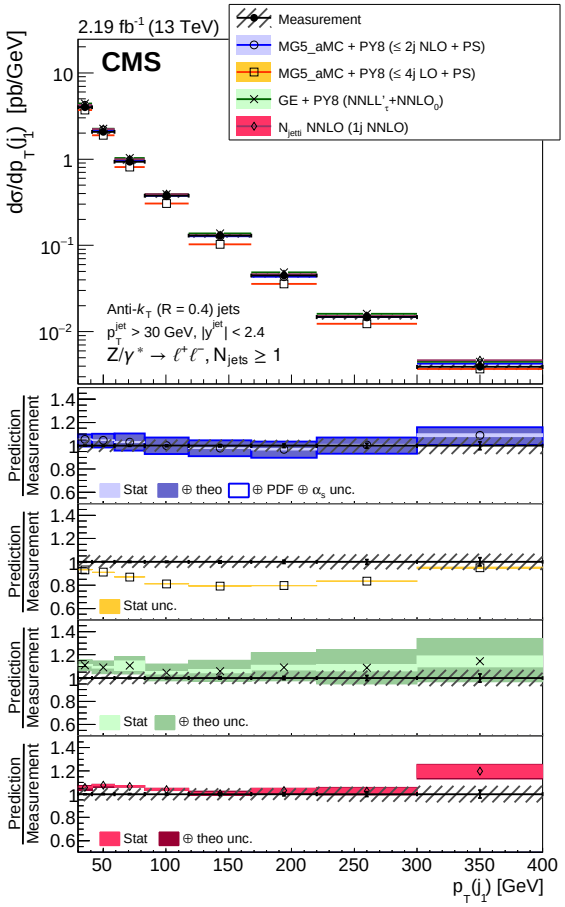

Figure 6: Measured cross section for Z + jets as a function of the transverse momentum of the first jet. Other details are as mentioned in the Fig. 4 caption.

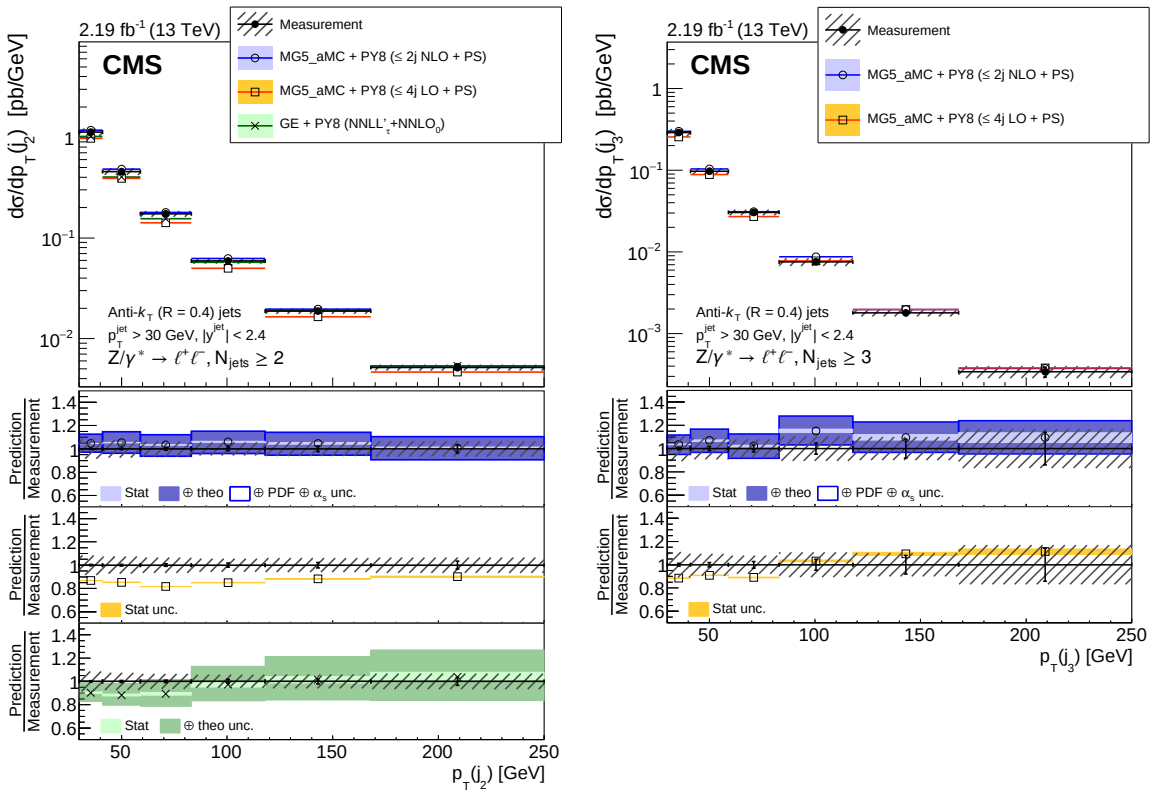

Figure 7: Measured cross section for Z + jets as a function of the transverse momentum of the second (left) and third (right) jet. Other details are as mentioned in the Fig. 4 caption.

high-$p_{\mathrm{T}}(\mathrm{Z})$ region, i.e. in the high jet multiplicity sample, the distribution is more symmetric. The NLO MG5_aMC prediction provides a better description of the JZB distribution than GENEVA and LO MG5_aMC. This applies to both configurations, JZB < 0 and > 0. This observation indicates that the NLO correction is important for the description of hadronic activity beyond the jet acceptance used in this analysis.

11 Summary

We have measured differential cross sections for the production of a Z boson in association with jets, where the Z boson decays into two charged leptons with $p_{\mathrm{T}} > 20\,\mathrm{GeV}$ and $|\eta| < 2.4$. The data sample corresponds to an integrated luminosity of $2.19\,\mathrm{fb}^{-1}$ collected with the CMS detector during the 2015 proton-proton LHC run at a centre-of-mass energy of 13 TeV.

The cross section has been measured as functions of the exclusive and inclusive jet multiplicities up to 6, of the transverse momentum of the Z boson, jet kinematic variables including jet transverse momentum (p_{T}), the scalar sum of jet transverse momenta (H_{T}), and the jet rapidity (y) for inclusive jet multiplicities of 1, 2, and 3. The balance in transverse momentum between the reconstructed jet recoil and the Z boson has been measured for different jet multiplicities. This balance has also been measured separating events with a recoil smaller and larger than the boson p_{T} using the JZB variable. Jets with $p_{\mathrm{T}} > 30\,\mathrm{GeV}$ and $|y| < 2.4$ are used in the definition of the different jet quantities.

The results are compared to the predictions of four different calculations. The first two merge matrix elements with different final-state parton multiplicities. The first is LO for multiplicities

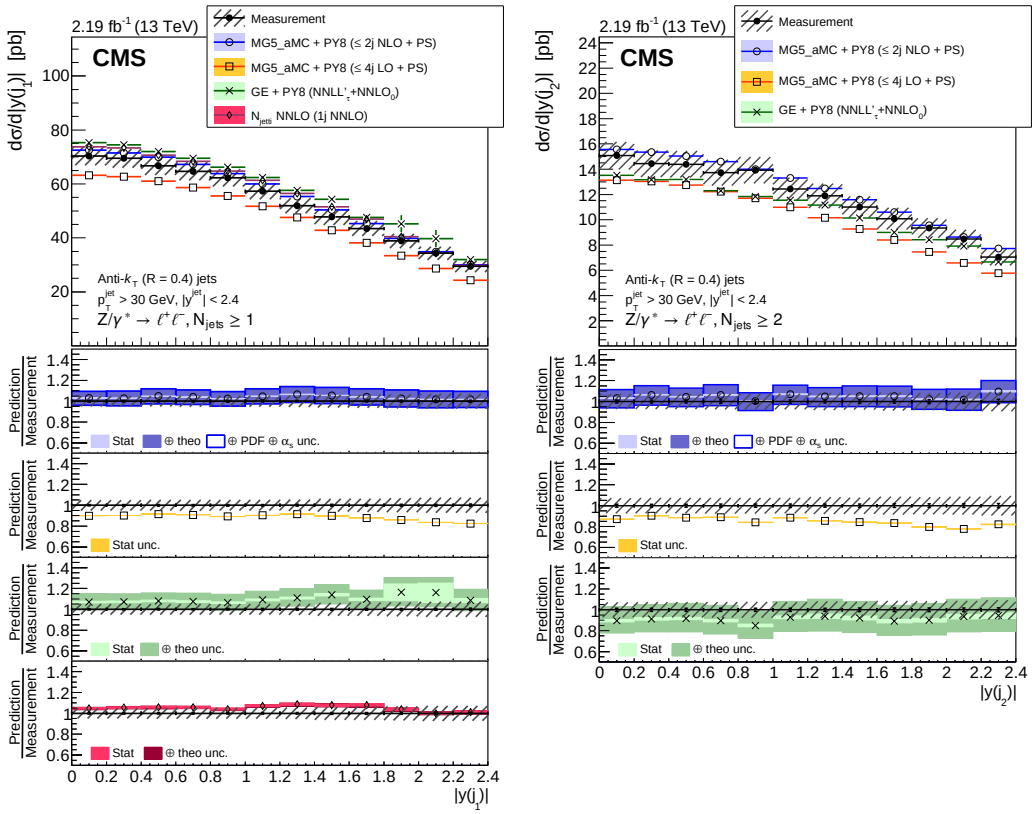

Figure 8: Measured cross section for Z + jets as a function of the absolute rapidity of the first (left) and second (right) jet. Other details are as mentioned in the Fig. 4 caption.

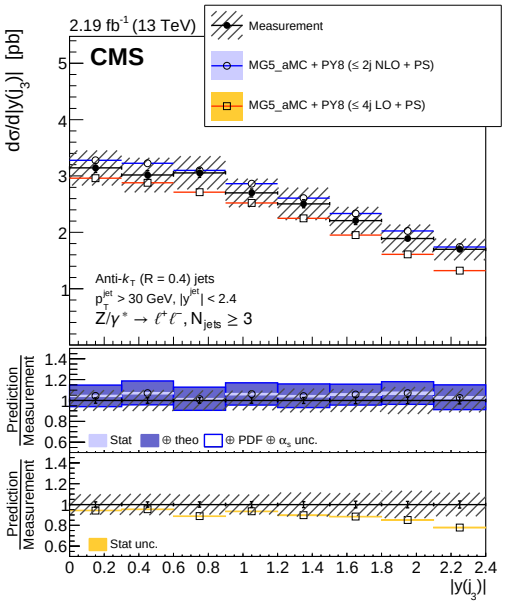

Figure 9: Measured cross section for Z + jets as a function of the absolute rapidity of the third jet. Other details are as mentioned in the Fig. 4 caption.

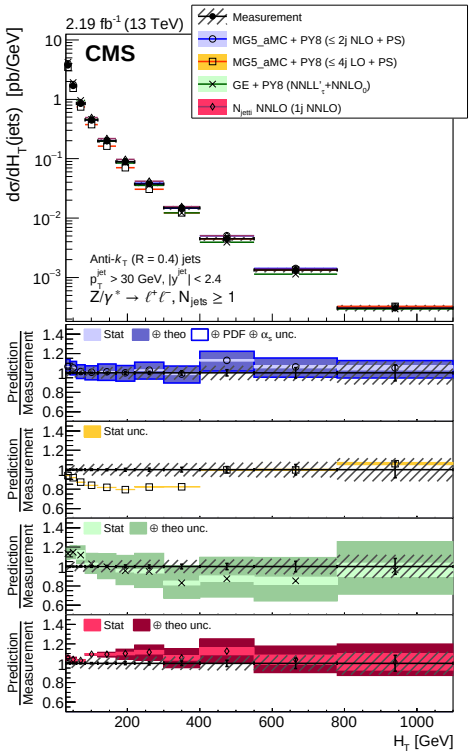

Figure 10: Measured cross section for Z + jets as a function of the H_T observable for events with at least one jet. Other details are as mentioned in the Fig. 4 caption.

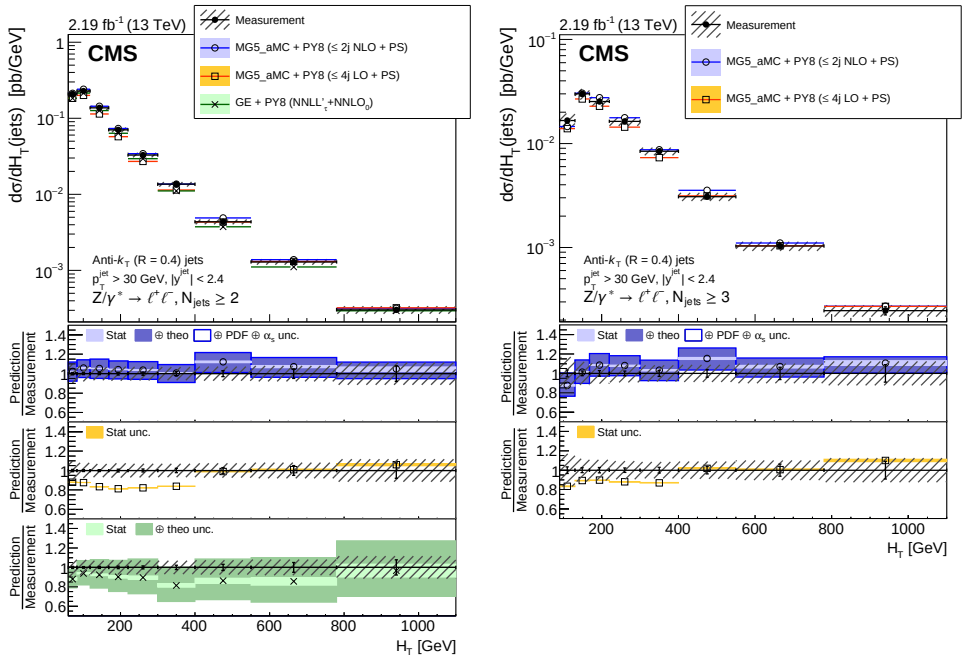

Figure 11: Measured cross section for Z + jets as a function of the H_T observable of jets for events with at least two (left) and three (right) jets. Other details are as mentioned in the Fig. 4 caption.

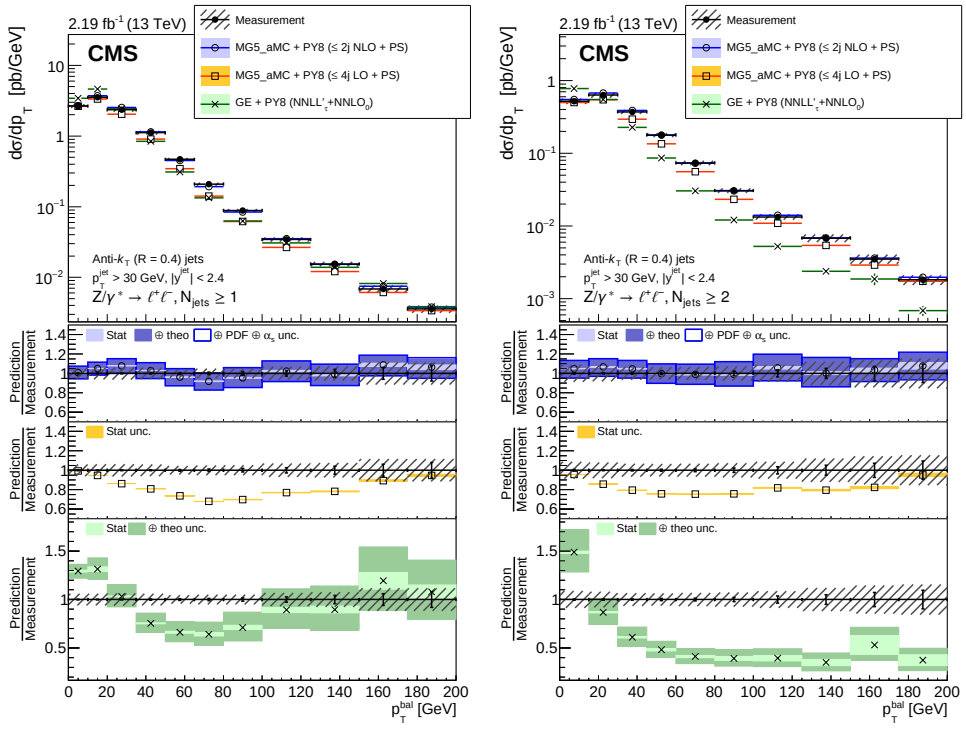

Figure 12: Measured cross section for Z + jets as a function of the transverse momentum balance between the Z boson and the accompanying jets for events with at least one (left) and two (right) jets. Other details are as mentioned in the Fig. 4 caption.

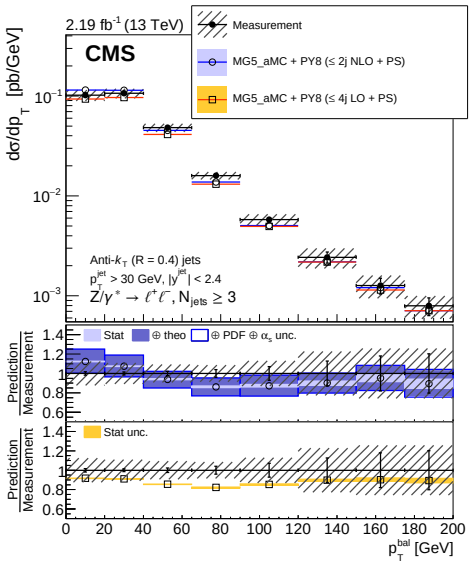

Figure 13: Measured cross section for Z + jets as a function of the transverse momentum balance between the Z boson and the accompanying jets for events with at least three jets. Other details are as mentioned in the Fig. 4 caption.

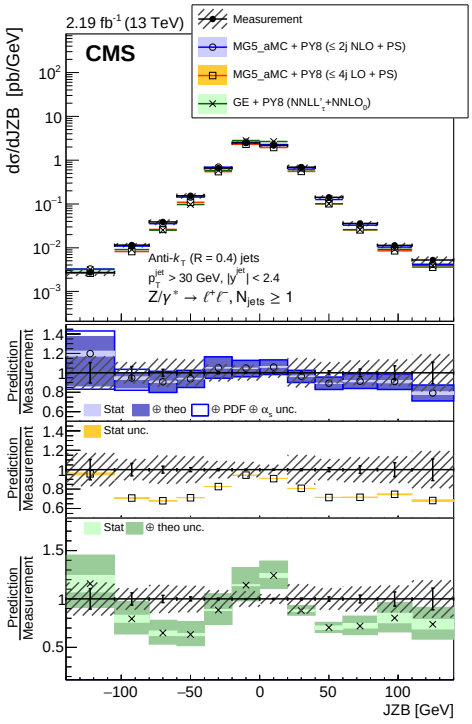

Figure 14: Measured cross section for Z + jets as a function of the JZB variable (see text), with no restriction on $p_T(Z)$. Other details are as mentioned in the Fig. 4 caption.

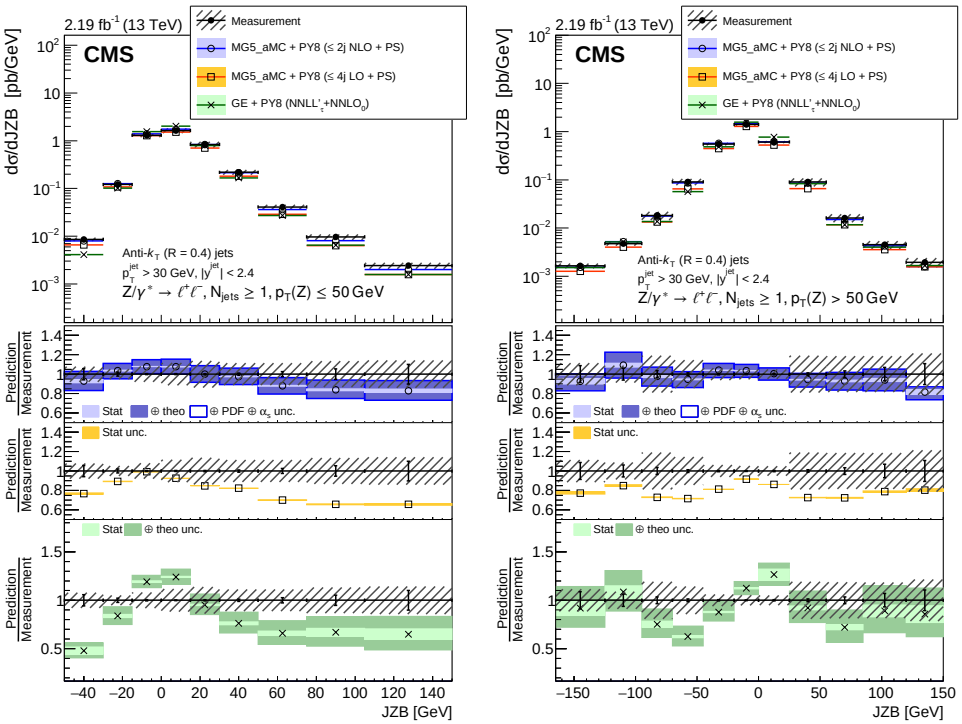

Figure 15: Measured cross section for Z + jets as a function of the JZB variable (see text), for $p_T(Z) < 50$ GeV (left) and $p_T(Z) > 50$ GeV (right). Other details are as mentioned in the Fig. 4 caption.

up to 4, the second NLO for multiplicities up to 2 and LO for a jet multiplicity of 3, and both are based on MG5_aMC. The third is a combination of NNLO calculation with NNLL resummation, based on GENEVA. The fourth is a fixed order NNLO calculation of one Z boson and one jet. The first three calculations include parton showering, based on PYTHIA8.

The measurements are in good agreement with the results of the NLO multiparton calculation. Even the measurements for events with more than 2 jets agree within the $\approx 10\%$ measurement and 10% theoretical uncertainties, although this part of the calculation is only LO. The multiparton LO prediction does not agree as well as the NLO multiparton one. It exhibits significant discrepancies with data in jet multiplicity and in both transverse momentum and rapidity distributions of the leading jet.

The transverse momentum balance between the Z boson and the hadronic recoil, which is expected to be sensitive to soft-gluon radiation, has been measured for the first time at the LHC. The multiparton LO prediction fails to describe the measurement, while the multiparton NLO prediction provides a very good description for jet multiplicities computed with NLO accuracy.

Inclusive measurement for events with at least one jet are compared with the NNLO Z$+ \geq 1$ jet fixed order calculation. The agreement is good, even for the H_{T} observable, which is sensitive to events of different jet multiplicities.

The NNLO+NNLL predictions provide similar agreement for the measurements of the kinematic variables of the two leading jets, but fail to describe observables sensitive to extra jets. At low transverse momentum of the Z boson, the NLO multiparton calculation provides a better description than the NNLO+NNLL calculation, whereas both calculations provide a similar description at high transverse momentum.

The results suggest using multiparton NLO predictions for the estimation of the $\mathrm{Z} +$ jets contribution at the LHC in measurements and searches, and its associated uncertainty.

Acknowledgments

We congratulate our colleagues in the CERN accelerator departments for the excellent performance of the LHC and thank the technical and administrative staffs at CERN and at other CMS institutes for their contributions to the success of the CMS effort. In addition, we gratefully acknowledge the computing centres and personnel of the Worldwide LHC Computing Grid for delivering so effectively the computing infrastructure essential to our analyses. Finally, we acknowledge the enduring support for the construction and operation of the LHC and the CMS detector provided by the following funding agencies: the Austrian Federal Ministry of Science, Research and Economy and the Austrian Science Fund; the Belgian Fonds de la Recherche Scientifique, and Fonds voor Wetenschappelijk Onderzoek; the Brazilian Funding Agencies (CNPq, CAPES, FAPERJ, and FAPESP); the Bulgarian Ministry of Education and Science; CERN; the Chinese Academy of Sciences, Ministry of Science and Technology, and National Natural Science Foundation of China; the Colombian Funding Agency (COLCIENCIAS); the Croatian Ministry of Science, Education and Sport, and the Croatian Science Foundation; the Research Promotion Foundation, Cyprus; the Secretariat for Higher Education, Science, Technology and Innovation, Ecuador; the Ministry of Education and Research, Estonian Research Council via IUT23-4 and IUT23-6 and European Regional Development Fund, Estonia; the Academy of Finland, Finnish Ministry of Education and Culture, and Helsinki Institute of Physics; the Institut National de Physique Nucléaire et de Physique des Particules / CNRS, and

Commissariat à l'Énergie Atomique et aux Énergies Alternatives / CEA, France; the Bundesministerium für Bildung und Forschung, Deutsche Forschungsgemeinschaft, and Helmholtz-Gemeinschaft Deutscher Forschungszentren, Germany; the General Secretariat for Research and Technology, Greece; the National Research, Development and Innovation Fund, Hungary; the Department of Atomic Energy and the Department of Science and Technology, India; the Institute for Studies in Theoretical Physics and Mathematics, Iran; the Science Foundation, Ireland; the Istituto Nazionale di Fisica Nucleare, Italy; the Ministry of Science, ICT and Future Planning, and National Research Foundation (NRF), Republic of Korea; the Lithuanian Academy of Sciences; the Ministry of Education, and University of Malaya (Malaysia); the Mexican Funding Agencies (BUAP, CINVESTAV, CONACYT, LNS, SEP, and UASLP-FAI); the Ministry of Business, Innovation and Employment, New Zealand; the Pakistan Atomic Energy Commission; the Ministry of Science and Higher Education and the National Science Centre, Poland; the Fundação para a Ciência e a Tecnologia, Portugal; JINR, Dubna; the Ministry of Education and Science of the Russian Federation, the Federal Agency of Atomic Energy of the Russian Federation, Russian Academy of Sciences, the Russian Foundation for Basic Research and the Russian Competitiveness Program of NRNU "MEPhI"; the Ministry of Education, Science and Technological Development of Serbia; the Secretaría de Estado de Investigación, Desarrollo e Innovación, Programa Consolider-Ingenio 2010, Plan Estatal de Investigación Científica y Técnica y de Innovación 2013-2016, Plan de Ciencia, Tecnología e Innovación 2013-2017 del Principado de Asturias and Fondo Europeo de Desarrollo Regional, Spain; the Swiss Funding Agencies (ETH Board, ETH Zurich, PSI, SNF, UniZH, Canton Zurich, and SER); the Ministry of Science and Technology, Taipei; the Thailand Center of Excellence in Physics, the Institute for the Promotion of Teaching Science and Technology of Thailand, Special Task Force for Activating Research and the National Science and Technology Development Agency of Thailand; the Scientific and Technical Research Council of Turkey, and Turkish Atomic Energy Authority; the National Academy of Sciences of Ukraine, and State Fund for Fundamental Researches, Ukraine; the Science and Technology Facilities Council, UK; the US Department of Energy, and the US National Science Foundation.

Individuals have received support from the Marie-Curie programme and the European Research Council and Horizon 2020 Grant, contract No. 675440 (European Union); the Leventis Foundation; the A. P. Sloan Foundation; the Alexander von Humboldt Foundation; the Belgian Federal Science Policy Office; the Fonds pour la Formation à la Recherche dans l'Industrie et dans l'Agriculture (FRIA-Belgium); the Agentschap voor Innovatie door Wetenschap en Technologie (IWT-Belgium); the F.R.S.-FNRS and FWO (Belgium) under the "Excellence of Science - EOS" - be.h project n. 30820817; the Ministry of Education, Youth and Sports (MEYS) of the Czech Republic; the Lendület ("Momentum") Programme and the János Bolyai Research Scholarship of the Hungarian Academy of Sciences, the New National Excellence Program ÚNKP, the NKFIA research grants 123842, 123959, 124845, 124850 and 125105 (Hungary); the Council of Scientific and Industrial Research, India; the HOMING PLUS programme of the Foundation for Polish Science, cofinanced from European Union, Regional Development Fund, the Mobility Plus programme of the Ministry of Science and Higher Education, the National Science Center (Poland), contracts Harmonia 2014/14/M/ST2/00428, Opus 2014/13/B/ST2/02543, 2014/15/B/ST2/03998, and 2015/19/B/ST2/02861, Sonata-bis 2012/07/E/ST2/01406; the National Priorities Research Program by Qatar National Research Fund; the Programa de Excelencia María de Maeztu and the Programa Severo Ochoa del Principado de Asturias; the Thalis and Aristeia programmes cofinanced by EU-ESF and the Greek NSRF; the Rachadapisek Sompot Fund for Postdoctoral Fellowship, Chulalongkorn University and the Chulalongkorn Academic into Its 2nd Century Project Advancement Project (Thailand); the Welch Foundation, contract C-1845; and the Weston Havens Foundation (USA).

References

[1] ATLAS Collaboration, "Measurement of the production cross section of jets in association with a Z boson in pp collisions at $\sqrt{s} = 7$ TeV with the ATLAS detector", *JHEP* **07** (2013) 032, doi:10.1007/JHEP07(2013)032, arXiv:1304.7098.

[2] ATLAS Collaboration, "Measurement of the production cross section for Z/γ^* in association with jets in pp collisions at $\sqrt{s} = 7$ TeV with the ATLAS detector", *Phys. Rev. D* **85** (2012) 032009, doi:10.1103/PhysRevD.85.032009, arXiv:1111.2690.

[3] CMS Collaboration, "Jet production rates in association with W and Z bosons in pp collisions at $\sqrt{s} = 7$ TeV", *JHEP* **01** (2012) 010, doi:10.1007/JHEP01(2012)010, arXiv:1110.3226.

[4] CMS Collaboration, "Measurements of jet multiplicity and differential production cross sections of Z + jets events in proton-proton collisions at $\sqrt{s} = 7$ TeV", *Phys. Rev. D* **91** (2015) 052008, doi:10.1103/PhysRevD.91.052008, arXiv:1408.3104.

[5] CMS Collaboration, "Comparison of the Z/γ^* + jets to γ + jets cross sections in pp collisions at $\sqrt{s} = 8$ TeV", *JHEP* **10** (2015) 128, doi:10.1007/JHEP10(2015)128, arXiv:1505.06520. [Erratum: doi:10.1007/JHEP04(2016)010].

[6] CMS Collaboration, "Measurements of differential production cross sections for a Z boson in association with jets in pp collisions at $\sqrt{s} = 8$ TeV", *JHEP* **04** (2017) 022, doi:10.1007/JHEP04(2017)022, arXiv:1611.03844.

[7] LHCb Collaboration, "Measurement of forward W and Z boson production in association with jets in proton-proton collisions at $\sqrt{s} = 8$ TeV", *JHEP* **05** (2016) 131, doi:10.1007/JHEP05(2016)131, arXiv:1605.00951.

[8] ATLAS Collaboration, "Measurements of the production cross section of a Z boson in association with jets in pp collisions at $\sqrt{s} = 13$ TeV with the ATLAS detector", *Eur. Phys. J. C* **77** (2017) 361, doi:10.1140/epjc/s10052-017-4900-z, arXiv:1702.05725.

[9] CDF Collaboration, "Measurement of inclusive jet cross sections in $Z/\gamma^* \to e^+ e^-$ + jets production in $p\bar{p}$ collisions at $\sqrt{s} = 1.96$ TeV", *Phys. Rev. Lett.* **100** (2008) 102001, doi:10.1103/PhysRevLett.100.102001, arXiv:0711.3717.

[10] D0 Collaboration, "Measurement of differential Z/γ^* + jet + X cross sections in $p\bar{p}$ collisions at $\sqrt{s} = 1.96$ TeV", *Phys. Lett. B* **669** (2008) 278, doi:10.1016/j.physletb.2008.09.060, arXiv:0808.1296.

[11] CMS Collaboration, "Performance of electron reconstruction and selection with the CMS detector in proton-proton collisions at $\sqrt{s} = 8$ TeV", *JINST* **10** (2015) P06005, doi:10.1088/1748-0221/10/06/P06005, arXiv:1502.02701.

[12] CMS Collaboration, "Performance of CMS muon reconstruction in pp collision events at $\sqrt{s} = 7$ TeV", *JINST* **7** (2012) P10002, doi:10.1088/1748-0221/7/10/P10002, arXiv:1206.4071.

[13] CMS Collaboration, "The CMS trigger system", *JINST* **12** (2017) P01020, doi:10.1088/1748-0221/12/01/P01020, arXiv:1609.02366.

[14] F. De Almeida Dias, E. Nurse, and G. Hesketh, "LO versus NLO comparisons for Z + jets: MC as a tool for background determination for NP searches at LHC", (2011). arXiv:1102.0917.

[15] CMS Collaboration, "Search for physics beyond the standard model in events with a Z boson, jets, and missing transverse energy in pp collisions at $\sqrt{s} = 7$ TeV", *Phys. Lett. B* **716** (2012) 260, doi:10.1016/j.physletb.2012.08.026, arXiv:1204.3774.

[16] Y. L. Dokshitzer, D. Diakonov, and S. I. Troian, "On the transverse momentum distribution of massive lepton pairs", *Phys. Lett. B* **79** (1978) 269, doi:10.1016/0370-2693(78)90240-X.

[17] J. C. Collins, D. E. Soper, and G. F. Sterman, "Transverse momentum distribution in Drell–Yan pair and W and Z boson production", *Nucl. Phys. B* **250** (1985) 199, doi:10.1016/0550-3213(85)90479-1.

[18] J. Alwall et al., "The automated computation of tree-level and next-to-leading order differential cross sections, and their matching to parton shower simulations", *JHEP* **07** (2014) 079, doi:10.1007/JHEP07(2014)079, arXiv:1405.0301.

[19] T. Sjöstrand et al., "An introduction to PYTHIA 8.2", *Comput. Phys. Commun.* **191** (2015) 159, doi:10.1016/j.cpc.2015.01.024, arXiv:1410.3012.

[20] CMS Collaboration, "Event generator tunes obtained from underlying event and multiparton scattering measurements", *Eur. Phys. J. C* **76** (2016) 155, doi:10.1140/epjc/s10052-016-3988-x, arXiv:1512.00815.

[21] R. D. Ball et al., "Parton distributions with LHC data", *Nucl. Phys. B* **867** (2013) 244, doi:10.1016/j.nuclphysb.2012.10.003, arXiv:1207.1303.

[22] J. Alwall et al., "Comparative study of various algorithms for the merging of parton showers and matrix elements in hadronic collisions", *Eur. Phys. J. C* **53** (2008) 473, doi:10.1140/epjc/s10052-007-0490-5, arXiv:0706.2569.

[23] J. Alwall, S. de Visscher, and F. Maltoni, "QCD radiation in the production of heavy colored particles at the LHC", *JHEP* **02** (2009) 017, doi:10.1088/1126-6708/2009/02/017, arXiv:0810.5350.

[24] NNPDF Collaboration, "Parton distributions for the LHC run II", *JHEP* **04** (2015) 040, doi:10.1007/JHEP04(2015)040, arXiv:1410.8849.

[25] R. Frederix and S. Frixione, "Merging meets matching in MC@NLO", *JHEP* **12** (2012) 061, doi:10.1007/JHEP12(2012)061, arXiv:1209.6215.

[26] S. Alioli et al., "Drell–Yan production at NNLL'+NNLO matched to parton showers", *Phys. Rev. D* **92** (2015) 094020, doi:10.1103/PhysRevD.92.094020, arXiv:1508.01475.

[27] S. Alioli et al., "Combining Higher-Order Resummation with Multiple NLO Calculations and Parton Showers in GENEVA", *JHEP* **09** (2013) 120, doi:10.1007/JHEP09(2013)120, arXiv:1211.7049.

[28] I. W. Stewart, F. J. Tackmann, and W. J. Waalewijn, "N-jettiness: An inclusive event shape to veto jets", *Phys. Rev. Lett.* **105** (2010) 092002, doi:10.1103/PhysRevLett.105.092002, arXiv:1004.2489.

[29] J. Butterworth et al., "PDF4LHC recommendations for LHC run II", *J. Phys G.* **43** (2016) 023001, doi:10.1088/0954-3899/43/2/023001, arXiv:1510.03865.

[30] R. Boughezal, X. Liu, and F. Petriello, "Phenomenology of the Z-boson plus jet process at NNLO", *Phys. Rev. D* **94** (2016) 074015, doi:10.1103/PhysRevD.94.074015, arXiv:1602.08140.

[31] R. Boughezal et al., "Z boson production in association with a jet at next-to-next-to-leading order in perturbative QCD", *Phys. Rev. Lett.* **116** (2016) 152001, doi:10.1103/PhysRevLett.116.152001, arXiv:1512.01291.

[32] S. Dulat et al., "New parton distribution functions from a global analysis of quantum chromodynamics", *Phys. Rev. D* **93** (2016) 033006, doi:10.1103/PhysRevD.93.033006, arXiv:1506.07443.

[33] K. Melnikov and F. Petriello, "Electroweak gauge boson production at hadron colliders through $O(\alpha_s^2)$", *Phys. Rev. D* **74** (2006) 114017, doi:10.1103/PhysRevD.74.114017, arXiv:hep-ph/0609070.

[34] R. Abbate et al., "Thrust at N^{3}LL with Power Corrections and a Precision Global Fit for $\alpha_s(m_Z)$", *Phys. Rev. D* **83** (2011) 074021, doi:10.1103/PhysRevD.83.074021, arXiv:1006.3080.

[35] Z. Ligeti, I. W. Stewart, and F. J. Tackmann, "Treating the b quark distribution function with reliable uncertainties", *Phys. Rev. D* **78** (2008) 114014, doi:10.1103/PhysRevD.78.114014, arXiv:0807.1926.

[36] R. Frederix et al., "Four-lepton production at hadron colliders: aMC@NLO predictions with theoretical uncertainties", *JHEP* **02** (2012) 099, doi:10.1007/JHEP02(2012)099, arXiv:1110.4738.

[37] GEANT4 Collaboration, "GEANT4—a simulation toolkit", *Nucl. Instrum. Meth. A* **506** (2003) 250, doi:10.1016/S0168-9002(03)01368-8.

[38] P. Nason, "A new method for combining NLO QCD with shower Monte Carlo algorithms", *JHEP* **11** (2004) 040, doi:10.1088/1126-6708/2004/11/040, arXiv:hep-ph/0409146.

[39] S. Frixione, P. Nason, and C. Oleari, "Matching NLO QCD computations with parton shower simulations: the POWHEG method", *JHEP* **11** (2007) 070, doi:10.1088/1126-6708/2007/11/070, arXiv:0709.2092.

[40] S. Alioli, P. Nason, C. Oleari, and E. Re, "A general framework for implementing NLO calculations in shower Monte Carlo programs: the POWHEG BOX", *JHEP* **06** (2010) 043, doi:10.1007/JHEP06(2010)043, arXiv:1002.2581.

[41] S. Frixione, P. Nason, and G. Ridolfi, "A positive-weight next-to-leading-order Monte Carlo for heavy flavour hadroproduction", *JHEP* **09** (2007) 126, doi:10.1088/1126-6708/2007/09/126, arXiv:0707.3088.

[42] P. Nason and G. Zanderighi, "W^+W^-, WZ and ZZ production in the POWHEG-BOX-v2", *Eur. Phys. J. C* **74** (2014) 2702, doi:10.1140/epjc/s10052-013-2702-5, arXiv:1311.1365.

[43] CMS Collaboration, "Particle-flow reconstruction and global event description with the CMS detector", *JINST* **12** (2017) P10003, doi:10.1088/1748-0221/12/10/P10003, arXiv:1706.04965.

[44] M. Cacciari, G. P. Salam, and G. Soyez, "The anti-k_T jet clustering algorithm", *JHEP* **04** (2008) 063, doi:10.1088/1126-6708/2008/04/063, arXiv:0802.1189.

[45] M. Cacciari, G. P. Salam, and G. Soyez, "FastJet user manual", *Eur. Phys. J. C* **72** (2012) 1896, doi:10.1140/epjc/s10052-012-1896-2, arXiv:1111.6097.

[46] M. Cacciari and G. P. Salam, "Pileup subtraction using jet areas", *Phys. Lett. B* **659** (2008) 119, doi:10.1016/j.physletb.2007.09.077, arXiv:0707.1378.

[47] CMS Collaboration, "Determination of jet energy calibration and transverse momentum resolution in CMS", *JINST* **6** (2011) P11002, doi:10.1088/1748-0221/6/11/P11002, arXiv:1107.4277.

[48] CMS Collaboration, "Jet energy scale and resolution in the CMS experiment in pp collisions at 8 TeV", *JINST* **12** (2017) P02014, doi:10.1088/1748-0221/12/02/P02014, arXiv:1607.03663.

[49] CMS Collaboration, "Jet algorithms performance in 13 TeV data", CMS Physics Analysis Summary CMS-PAS-JME-16-003, CERN, 2013.

[50] CMS Collaboration, "Pileup jet identification", CMS Physics Analysis Summary CMS-PAS-JME-13-005, CERN, 2013.

[51] G. D'Agostini, "A multidimensional unfolding method based on Bayes' theorem", *Nucl. Instrum. Meth. A* **362** (1995) 487, doi:10.1016/0168-9002(95)00274-X.

[52] T. Adye, "Unfolding algorithms and tests using RooUnfold", in *Proceedings of the PHYSTAT 2011 Workshop, CERN, Geneva, Switzerland, January 2011, CERN-2011-006*, p. 313. 2011. arXiv:1105.1160.

[53] CMS Collaboration, "CMS luminosity measurement for the 2015 data taking period", CMS Physics Analysis Summary CMS-PAS-LUM-15-001, CERN, 2016.

A The CMS Collaboration

Yerevan Physics Institute, Yerevan, Armenia
A.M. Sirunyan, A. Tumasyan

Institut für Hochenergiephysik, Wien, Austria
W. Adam, F. Ambrogi, E. Asilar, T. Bergauer, J. Brandstetter, E. Brondolin, M. Dragicevic, J. Erö, A. Escalante Del Valle, M. Flechl, M. Friedl, R. Frühwirth[1], V.M. Ghete, J. Hrubec, M. Jeitler[1], N. Krammer, I. Krätschmer, D. Liko, T. Madlener, I. Mikulec, N. Rad, H. Rohringer, J. Schieck[1], R. Schöfbeck, M. Spanring, D. Spitzbart, A. Taurok, W. Waltenberger, J. Wittmann, C.-E. Wulz[1], M. Zarucki

Institute for Nuclear Problems, Minsk, Belarus
V. Chekhovsky, V. Mossolov, J. Suarez Gonzalez

Universiteit Antwerpen, Antwerpen, Belgium
E.A. De Wolf, D. Di Croce, X. Janssen, J. Lauwers, M. Pieters, M. Van De Klundert, H. Van Haevermaet, P. Van Mechelen, N. Van Remortel

Vrije Universiteit Brussel, Brussel, Belgium
S. Abu Zeid, F. Blekman, J. D'Hondt, I. De Bruyn, J. De Clercq, K. Deroover, G. Flouris, D. Lontkovskyi, S. Lowette, I. Marchesini, S. Moortgat, L. Moreels, Q. Python, K. Skovpen, S. Tavernier, W. Van Doninck, P. Van Mulders, I. Van Parijs

Université Libre de Bruxelles, Bruxelles, Belgium
D. Beghin, B. Bilin, H. Brun, B. Clerbaux, G. De Lentdecker, H. Delannoy, B. Dorney, G. Fasanella, L. Favart, R. Goldouzian, A. Grebenyuk, A.K. Kalsi, T. Lenzi, J. Luetic, T. Seva, E. Starling, C. Vander Velde, P. Vanlaer, D. Vannerom, Q. Wang

Ghent University, Ghent, Belgium
T. Cornelis, D. Dobur, A. Fagot, M. Gul, I. Khvastunov[2], D. Poyraz, C. Roskas, D. Trocino, M. Tytgat, W. Verbeke, B. Vermassen, M. Vit, N. Zaganidis

Université Catholique de Louvain, Louvain-la-Neuve, Belgium
H. Bakhshiansohi, O. Bondu, S. Brochet, G. Bruno, C. Caputo, P. David, C. Delaere, M. Delcourt, B. Francois, A. Giammanco, G. Krintiras, V. Lemaitre, A. Magitteri, A. Mertens, M. Musich, K. Piotrzkowski, A. Saggio, M. Vidal Marono, S. Wertz, J. Zobec

Centro Brasileiro de Pesquisas Fisicas, Rio de Janeiro, Brazil
W.L. Aldá Júnior, F.L. Alves, G.A. Alves, L. Brito, G. Correia Silva, C. Hensel, A. Moraes, M.E. Pol, P. Rebello Teles

Universidade do Estado do Rio de Janeiro, Rio de Janeiro, Brazil
E. Belchior Batista Das Chagas, W. Carvalho, J. Chinellato[3], E. Coelho, E.M. Da Costa, G.G. Da Silveira[4], D. De Jesus Damiao, S. Fonseca De Souza, H. Malbouisson, M. Medina Jaime[5], M. Melo De Almeida, C. Mora Herrera, L. Mundim, H. Nogima, L.J. Sanchez Rosas, A. Santoro, A. Sznajder, M. Thiel, E.J. Tonelli Manganote[3], F. Torres Da Silva De Araujo, A. Vilela Pereira

Universidade Estadual Paulista [a], Universidade Federal do ABC [b], São Paulo, Brazil
S. Ahuja[a], C.A. Bernardes[a], L. Calligaris[a], T.R. Fernandez Perez Tomei[a], E.M. Gregores[b], P.G. Mercadante[b], S.F. Novaes[a], Sandra S. Padula[a], D. Romero Abad[b], J.C. Ruiz Vargas[a]

Institute for Nuclear Research and Nuclear Energy, Bulgarian Academy of Sciences, Sofia,

Bulgaria
A. Aleksandrov, R. Hadjiiska, P. Iaydjiev, A. Marinov, M. Misheva, M. Rodozov, M. Shopova, G. Sultanov

University of Sofia, Sofia, Bulgaria
A. Dimitrov, L. Litov, B. Pavlov, P. Petkov

Beihang University, Beijing, China
W. Fang[6], X. Gao[6], L. Yuan

Institute of High Energy Physics, Beijing, China
M. Ahmad, J.G. Bian, G.M. Chen, H.S. Chen, M. Chen, Y. Chen, C.H. Jiang, D. Leggat, H. Liao, Z. Liu, F. Romeo, S.M. Shaheen, A. Spiezia, J. Tao, C. Wang, Z. Wang, E. Yazgan, H. Zhang, J. Zhao

State Key Laboratory of Nuclear Physics and Technology, Peking University, Beijing, China
Y. Ban, G. Chen, J. Li, Q. Li, S. Liu, Y. Mao, S.J. Qian, D. Wang, Z. Xu

Tsinghua University, Beijing, China
Y. Wang

Universidad de Los Andes, Bogota, Colombia
C. Avila, A. Cabrera, C.A. Carrillo Montoya, L.F. Chaparro Sierra, C. Florez, C.F. González Hernández, M.A. Segura Delgado

University of Split, Faculty of Electrical Engineering, Mechanical Engineering and Naval Architecture, Split, Croatia
B. Courbon, N. Godinovic, D. Lelas, I. Puljak, T. Sculac

University of Split, Faculty of Science, Split, Croatia
Z. Antunovic, M. Kovac

Institute Rudjer Boskovic, Zagreb, Croatia
V. Brigljevic, D. Ferencek, K. Kadija, B. Mesic, A. Starodumov[7], T. Susa

University of Cyprus, Nicosia, Cyprus
M.W. Ather, A. Attikis, G. Mavromanolakis, J. Mousa, C. Nicolaou, F. Ptochos, P.A. Razis, H. Rykaczewski

Charles University, Prague, Czech Republic
M. Finger[8], M. Finger Jr.[8]

Universidad San Francisco de Quito, Quito, Ecuador
E. Carrera Jarrin

Academy of Scientific Research and Technology of the Arab Republic of Egypt, Egyptian Network of High Energy Physics, Cairo, Egypt
A. Mohamed[9], Y. Mohammed[10], E. Salama[11,12]

National Institute of Chemical Physics and Biophysics, Tallinn, Estonia
S. Bhowmik, A. Carvalho Antunes De Oliveira, R.K. Dewanjee, M. Kadastik, L. Perrini, M. Raidal, C. Veelken

Department of Physics, University of Helsinki, Helsinki, Finland
P. Eerola, H. Kirschenmann, J. Pekkanen, M. Voutilainen

Helsinki Institute of Physics, Helsinki, Finland
J. Havukainen, J.K. Heikkilä, T. Järvinen, V. Karimäki, R. Kinnunen, T. Lampén, K. Lassila-Perini, S. Laurila, S. Lehti, T. Lindén, P. Luukka, T. Mäenpää, H. Siikonen, E. Tuominen, J. Tuominiemi

Lappeenranta University of Technology, Lappeenranta, Finland
T. Tuuva

IRFU, CEA, Université Paris-Saclay, Gif-sur-Yvette, France
M. Besancon, F. Couderc, M. Dejardin, D. Denegri, J.L. Faure, F. Ferri, S. Ganjour, A. Givernaud, P. Gras, G. Hamel de Monchenault, P. Jarry, C. Leloup, E. Locci, M. Machet, J. Malcles, G. Negro, J. Rander, A. Rosowsky, M.Ö. Sahin, M. Titov

Laboratoire Leprince-Ringuet, Ecole polytechnique, CNRS/IN2P3, Université Paris-Saclay, Palaiseau, France
A. Abdulsalam[13], C. Amendola, I. Antropov, S. Baffioni, F. Beaudette, P. Busson, L. Cadamuro, C. Charlot, R. Granier de Cassagnac, M. Jo, I. Kucher, S. Lisniak, A. Lobanov, J. Martin Blanco, M. Nguyen, C. Ochando, G. Ortona, P. Paganini, P. Pigard, R. Salerno, J.B. Sauvan, Y. Sirois, A.G. Stahl Leiton, Y. Yilmaz, A. Zabi, A. Zghiche

Université de Strasbourg, CNRS, IPHC UMR 7178, F-67000 Strasbourg, France
J.-L. Agram[14], J. Andrea, D. Bloch, J.-M. Brom, E.C. Chabert, C. Collard, E. Conte[14], X. Coubez, F. Drouhin[14], J.-C. Fontaine[14], D. Gelé, U. Goerlach, M. Jansová, P. Juillot, A.-C. Le Bihan, N. Tonon, P. Van Hove

Centre de Calcul de l'Institut National de Physique Nucleaire et de Physique des Particules, CNRS/IN2P3, Villeurbanne, France
S. Gadrat

Université de Lyon, Université Claude Bernard Lyon 1, CNRS-IN2P3, Institut de Physique Nucléaire de Lyon, Villeurbanne, France
S. Beauceron, C. Bernet, G. Boudoul, N. Chanon, R. Chierici, D. Contardo, P. Depasse, H. El Mamouni, J. Fay, L. Finco, S. Gascon, M. Gouzevitch, G. Grenier, B. Ille, F. Lagarde, I.B. Laktineh, H. Lattaud, M. Lethuillier, L. Mirabito, A.L. Pequegnot, S. Perries, A. Popov[15], V. Sordini, M. Vander Donckt, S. Viret, S. Zhang

Georgian Technical University, Tbilisi, Georgia
T. Toriashvili[16]

Tbilisi State University, Tbilisi, Georgia
Z. Tsamalaidze[8]

RWTH Aachen University, I. Physikalisches Institut, Aachen, Germany
C. Autermann, L. Feld, M.K. Kiesel, K. Klein, M. Lipinski, M. Preuten, M.P. Rauch, C. Schomakers, J. Schulz, M. Teroerde, B. Wittmer, V. Zhukov[15]

RWTH Aachen University, III. Physikalisches Institut A, Aachen, Germany
A. Albert, D. Duchardt, M. Endres, M. Erdmann, S. Erdweg, T. Esch, R. Fischer, S. Ghosh, A. Güth, T. Hebbeker, C. Heidemann, K. Hoepfner, S. Knutzen, M. Merschmeyer, A. Meyer, P. Millet, S. Mukherjee, T. Pook, M. Radziej, H. Reithler, M. Rieger, F. Scheuch, D. Teyssier, S. Thüer

RWTH Aachen University, III. Physikalisches Institut B, Aachen, Germany
G. Flügge, B. Kargoll, T. Kress, A. Künsken, T. Müller, A. Nehrkorn, A. Nowack, C. Pistone, O. Pooth, A. Stahl[17]

Deutsches Elektronen-Synchrotron, Hamburg, Germany
M. Aldaya Martin, T. Arndt, C. Asawatangtrakuldee, I. Babounikau, K. Beernaert, O. Behnke, U. Behrens, A. Bermúdez Martínez, D. Bertsche, A.A. Bin Anuar, K. Borras[18], V. Botta, A. Campbell, P. Connor, C. Contreras-Campana, F. Costanza, V. Danilov, A. De Wit, M.M. Defranchis, C. Diez Pardos, D. Domínguez Damiani, G. Eckerlin, D. Eckstein, T. Eichhorn, A. Elwood, E. Eren, E. Gallo[19], A. Geiser, J.M. Grados Luyando, A. Grohsjean, P. Gunnellini, M. Guthoff, A. Harb, J. Hauk, H. Jung, M. Kasemann, J. Keaveney, C. Kleinwort, J. Knolle, D. Krücker, W. Lange, A. Lelek, T. Lenz, K. Lipka, W. Lohmann[20], R. Mankel, I.-A. Melzer-Pellmann, A.B. Meyer, M. Meyer, M. Missiroli, G. Mittag, J. Mnich, A. Mussgiller, S.K. Pflitsch, D. Pitzl, A. Raspereza, M. Savitskyi, P. Saxena, P. Schütze, C. Schwanenberger, R. Shevchenko, A. Singh, N. Stefaniuk, H. Tholen, G.P. Van Onsem, R. Walsh, Y. Wen, K. Wichmann, C. Wissing, O. Zenaiev

University of Hamburg, Hamburg, Germany
R. Aggleton, S. Bein, A. Benecke, V. Blobel, M. Centis Vignali, T. Dreyer, E. Garutti, D. Gonzalez, J. Haller, A. Hinzmann, M. Hoffmann, A. Karavdina, G. Kasieczka, R. Klanner, R. Kogler, N. Kovalchuk, S. Kurz, V. Kutzner, J. Lange, D. Marconi, J. Multhaup, M. Niedziela, D. Nowatschin, T. Peiffer, A. Perieanu, A. Reimers, O. Rieger, C. Scharf, P. Schleper, A. Schmidt, S. Schumann, J. Schwandt, J. Sonneveld, H. Stadie, G. Steinbrück, F.M. Stober, M. Stöver, D. Troendle, E. Usai, A. Vanhoefer, B. Vormwald

Institut für Experimentelle Teilchenphysik, Karlsruhe, Germany
M. Akbiyik, C. Barth, M. Baselga, S. Baur, E. Butz, R. Caspart, T. Chwalek, F. Colombo, W. De Boer, A. Dierlamm, N. Faltermann, B. Freund, R. Friese, M. Giffels, M.A. Harrendorf, F. Hartmann[17], S.M. Heindl, U. Husemann, F. Kassel[17], S. Kudella, H. Mildner, M.U. Mozer, Th. Müller, M. Plagge, G. Quast, K. Rabbertz, M. Schröder, I. Shvetsov, G. Sieber, H.J. Simonis, R. Ulrich, S. Wayand, M. Weber, T. Weiler, S. Williamson, C. Wöhrmann, R. Wolf

Institute of Nuclear and Particle Physics (INPP), NCSR Demokritos, Aghia Paraskevi, Greece
G. Anagnostou, G. Daskalakis, T. Geralis, A. Kyriakis, D. Loukas, G. Paspalaki, I. Topsis-Giotis

National and Kapodistrian University of Athens, Athens, Greece
G. Karathanasis, S. Kesisoglou, A. Panagiotou, N. Saoulidou, E. Tziaferi, K. Vellidis

National Technical University of Athens, Athens, Greece
K. Kousouris, I. Papakrivopoulos

University of Ioánnina, Ioánnina, Greece
I. Evangelou, C. Foudas, P. Gianneios, P. Katsoulis, P. Kokkas, S. Mallios, N. Manthos, I. Papadopoulos, E. Paradas, J. Strologas, F.A. Triantis, D. Tsitsonis

MTA-ELTE Lendület CMS Particle and Nuclear Physics Group, Eötvös Loránd University, Budapest, Hungary
M. Csanad, N. Filipovic, G. Pasztor, O. Surányi, G.I. Veres

Wigner Research Centre for Physics, Budapest, Hungary
G. Bencze, C. Hajdu, D. Horvath[21], Á. Hunyadi, F. Sikler, V. Veszpremi, G. Vesztergombi[†], T.Á. Vámi

Institute of Nuclear Research ATOMKI, Debrecen, Hungary
N. Beni, S. Czellar, J. Karancsi[22], A. Makovec, J. Molnar, Z. Szillasi

Institute of Physics, University of Debrecen, Debrecen, Hungary
M. Bartók[23], P. Raics, Z.L. Trocsanyi, B. Ujvari

Indian Institute of Science (IISc), Bangalore, India
S. Choudhury, J.R. Komaragiri

National Institute of Science Education and Research, Bhubaneswar, India
S. Bahinipati[24], P. Mal, K. Mandal, A. Nayak[25], D.K. Sahoo[24], S.K. Swain

Panjab University, Chandigarh, India
S. Bansal, S.B. Beri, V. Bhatnagar, S. Chauhan, R. Chawla, N. Dhingra, R. Gupta, A. Kaur, M. Kaur, S. Kaur, R. Kumar, P. Kumari, M. Lohan, A. Mehta, S. Sharma, J.B. Singh, G. Walia

University of Delhi, Delhi, India
Ashok Kumar, Aashaq Shah, A. Bhardwaj, B.C. Choudhary, R.B. Garg, S. Keshri, A. Kumar, S. Malhotra, M. Naimuddin, K. Ranjan, R. Sharma

Saha Institute of Nuclear Physics, HBNI, Kolkata, India
R. Bhardwaj[26], R. Bhattacharya, S. Bhattacharya, U. Bhawandeep[26], D. Bhowmik, S. Dey, S. Dutt[26], S. Dutta, S. Ghosh, N. Majumdar, K. Mondal, S. Mukhopadhyay, S. Nandan, A. Purohit, P.K. Rout, A. Roy, S. Roy Chowdhury, S. Sarkar, M. Sharan, B. Singh, S. Thakur[26]

Indian Institute of Technology Madras, Madras, India
P.K. Behera

Bhabha Atomic Research Centre, Mumbai, India
R. Chudasama, D. Dutta, V. Jha, V. Kumar, A.K. Mohanty[17], P.K. Netrakanti, L.M. Pant, P. Shukla, A. Topkar

Tata Institute of Fundamental Research-A, Mumbai, India
T. Aziz, S. Dugad, B. Mahakud, S. Mitra, G.B. Mohanty, R. Ravindra Kumar Verma, N. Sur, B. Sutar

Tata Institute of Fundamental Research-B, Mumbai, India
S. Banerjee, S. Bhattacharya, S. Chatterjee, P. Das, M. Guchait, Sa. Jain, S. Kumar, M. Maity[27], G. Majumder, K. Mazumdar, N. Sahoo, T. Sarkar[27], N. Wickramage[28]

Indian Institute of Science Education and Research (IISER), Pune, India
S. Chauhan, S. Dube, V. Hegde, A. Kapoor, K. Kothekar, S. Pandey, A. Rane, S. Sharma

Institute for Research in Fundamental Sciences (IPM), Tehran, Iran
S. Chenarani[29], E. Eskandari Tadavani, S.M. Etesami[29], M. Khakzad, M. Mohammadi Najafabadi, M. Naseri, S. Paktinat Mehdiabadi[30], F. Rezaei Hosseinabadi, B. Safarzadeh[31], M. Zeinali

University College Dublin, Dublin, Ireland
M. Felcini, M. Grunewald

INFN Sezione di Bari [a], Università di Bari [b], Politecnico di Bari [c], Bari, Italy
M. Abbrescia[a,b], C. Calabria[a,b], A. Colaleo[a], D. Creanza[a,c], L. Cristella[a,b], N. De Filippis[a,c], M. De Palma[a,b], A. Di Florio[a,b], F. Errico[a,b], L. Fiore[a], A. Gelmi[a,b], G. Iaselli[a,c], S. Lezki[a,b], G. Maggi[a,c], M. Maggi[a], G. Miniello[a,b], S. My[a,b], S. Nuzzo[a,b], A. Pompili[a,b], G. Pugliese[a,c], R. Radogna[a], A. Ranieri[a], G. Selvaggi[a,b], A. Sharma[a], L. Silvestris[a,17], R. Venditti[a], P. Verwilligen[a], G. Zito[a]

INFN Sezione di Bologna [a], Università di Bologna [b], Bologna, Italy
G. Abbiendi[a], C. Battilana[a,b], D. Bonacorsi[a,b], L. Borgonovi[a,b], S. Braibant-Giacomelli[a,b], L. Brigliadori[a,b], R. Campanini[a,b], P. Capiluppi[a,b], A. Castro[a,b], F.R. Cavallo[a], S.S. Chhibra[a,b], G. Codispoti[a,b], M. Cuffiani[a,b], G.M. Dallavalle[a], F. Fabbri[a], A. Fanfani[a,b], D. Fasanella[a,b], P. Giacomelli[a], C. Grandi[a], L. Guiducci[a,b], S. Marcellini[a], G. Masetti[a], A. Montanari[a], F.L. Navarria[a,b], A. Perrotta[a], A.M. Rossi[a,b], T. Rovelli[a,b], G.P. Siroli[a,b], N. Tosi[a]

INFN Sezione di Catania [a], Università di Catania [b], Catania, Italy
S. Albergo[a,b], S. Costa[a,b], A. Di Mattia[a], F. Giordano[a,b], R. Potenza[a,b], A. Tricomi[a,b], C. Tuve[a,b]

INFN Sezione di Firenze [a], Università di Firenze [b], Firenze, Italy
G. Barbagli[a], K. Chatterjee[a,b], V. Ciulli[a,b], C. Civinini[a], R. D'Alessandro[a,b], E. Focardi[a,b], G. Latino, P. Lenzi[a,b], M. Meschini[a], S. Paoletti[a], L. Russo[a,32], G. Sguazzoni[a], D. Strom[a], L. Viliani[a]

INFN Laboratori Nazionali di Frascati, Frascati, Italy
L. Benussi, S. Bianco, F. Fabbri, D. Piccolo, F. Primavera[17]

INFN Sezione di Genova [a], Università di Genova [b], Genova, Italy
V. Calvelli, F. Ferro[a], F. Ravera[a,b], E. Robutti[a], S. Tosi[a,b]

INFN Sezione di Milano-Bicocca [a], Università di Milano-Bicocca [b], Milano, Italy
A. Benaglia[a], A. Beschi[b], L. Brianza[a,b], F. Brivio[a,b], V. Ciriolo[a,b,17], M.E. Dinardo[a,b], S. Fiorendi[a,b], S. Gennai[a], A. Ghezzi[a,b], P. Govoni[a,b], M. Malberti[a,b], S. Malvezzi[a], R.A. Manzoni[a,b], D. Menasce[a], L. Moroni[a], M. Paganoni[a,b], K. Pauwels[a,b], D. Pedrini[a], S. Pigazzini[a,b,33], S. Ragazzi[a,b], T. Tabarelli de Fatis[a,b]

INFN Sezione di Napoli [a], Università di Napoli 'Federico II' [b], Napoli, Italy, Università della Basilicata [c], Potenza, Italy, Università G. Marconi [d], Roma, Italy
S. Buontempo[a], N. Cavallo[a,c], S. Di Guida[a,d,17], F. Fabozzi[a,c], F. Fienga[a,b], G. Galati[a,b], A.O.M. Iorio[a,b], W.A. Khan[a], L. Lista[a], S. Meola[a,d,17], P. Paolucci[a,17], C. Sciacca[a,b], F. Thyssen[a], E. Voevodina[a,b]

INFN Sezione di Padova [a], Università di Padova [b], Padova, Italy, Università di Trento [c], Trento, Italy
P. Azzi[a], N. Bacchetta[a], L. Benato[a,b], D. Bisello[a,b], A. Boletti[a,b], P. Checchia[a], M. Dall'Osso[a,b], P. De Castro Manzano[a], T. Dorigo[a], F. Gasparini[a,b], U. Gasparini[a,b], A. Gozzelino[a], S. Lacaprara[a], P. Lujan, M. Margoni[a,b], A.T. Meneguzzo[a,b], M. Passaseo[a], N. Pozzobon[a,b], P. Ronchese[a,b], R. Rossin[a,b], F. Simonetto[a,b], A. Tiko, E. Torassa[a], M. Zanetti[a,b], P. Zotto[a,b], G. Zumerle[a,b]

INFN Sezione di Pavia [a], Università di Pavia [b], Pavia, Italy
A. Braghieri[a], A. Magnani[a], P. Montagna[a,b], S.P. Ratti[a,b], V. Re[a], M. Ressegotti[a,b], C. Riccardi[a,b], P. Salvini[a], I. Vai[a,b], P. Vitulo[a,b]

INFN Sezione di Perugia [a], Università di Perugia [b], Perugia, Italy
L. Alunni Solestizi[a,b], M. Biasini[a,b], G.M. Bilei[a], C. Cecchi[a,b], D. Ciangottini[a,b], L. Fanò[a,b], P. Lariccia[a,b], R. Leonardi[a,b], E. Manoni[a], G. Mantovani[a,b], V. Mariani[a,b], M. Menichelli[a], A. Rossi[a,b], A. Santocchia[a,b], D. Spiga[a]

INFN Sezione di Pisa [a], Università di Pisa [b], Scuola Normale Superiore di Pisa [c], Pisa, Italy
K. Androsov[a], P. Azzurri[a], G. Bagliesi[a], L. Bianchini[a], T. Boccali[a], L. Borrello, R. Castaldi[a], M.A. Ciocci[a,b], R. Dell'Orso[a], G. Fedi[a], L. Giannini[a,c], A. Giassi[a], M.T. Grippo[a], F. Ligabue[a,c],

T. Lomtadze[a], E. Manca[a,c], G. Mandorli[a,c], A. Messineo[a,b], F. Palla[a], A. Rizzi[a,b], P. Spagnolo[a], R. Tenchini[a], G. Tonelli[a,b], A. Venturi[a], P.G. Verdini[a]

INFN Sezione di Roma [a], Sapienza Università di Roma [b], Rome, Italy
L. Barone[a,b], F. Cavallari[a], M. Cipriani[a,b], N. Daci[a], D. Del Re[a,b], E. Di Marco[a,b], M. Diemoz[a], S. Gelli[a,b], E. Longo[a,b], B. Marzocchi[a,b], P. Meridiani[a], G. Organtini[a,b], F. Pandolfi[a], R. Paramatti[a,b], F. Preiato[a,b], S. Rahatlou[a,b], C. Rovelli[a], F. Santanastasio[a,b]

INFN Sezione di Torino [a], Università di Torino [b], Torino, Italy, Università del Piemonte Orientale [c], Novara, Italy
N. Amapane[a,b], R. Arcidiacono[a,c], S. Argiro[a,b], M. Arneodo[a,c], N. Bartosik[a], R. Bellan[a,b], C. Biino[a], N. Cartiglia[a], R. Castello[a,b], F. Cenna[a,b], M. Costa[a,b], R. Covarelli[a,b], A. Degano[a,b], N. Demaria[a], B. Kiani[a,b], C. Mariotti[a], S. Maselli[a], E. Migliore[a,b], V. Monaco[a,b], E. Monteil[a,b], M. Monteno[a], M.M. Obertino[a,b], L. Pacher[a,b], N. Pastrone[a], M. Pelliccioni[a], G.L. Pinna Angioni[a,b], A. Romero[a,b], M. Ruspa[a,c], R. Sacchi[a,b], K. Shchelina[a,b], V. Sola[a], A. Solano[a,b], A. Staiano[a]

INFN Sezione di Trieste [a], Università di Trieste [b], Trieste, Italy
S. Belforte[a], V. Candelise[a,b], M. Casarsa[a], F. Cossutti[a], G. Della Ricca[a,b], F. Vazzoler[a,b], A. Zanetti[a]

Kyungpook National University
D.H. Kim, G.N. Kim, M.S. Kim, J. Lee, S. Lee, S.W. Lee, C.S. Moon, Y.D. Oh, S. Sekmen, D.C. Son, Y.C. Yang

Chonnam National University, Institute for Universe and Elementary Particles, Kwangju, Korea
H. Kim, D.H. Moon, G. Oh

Hanyang University, Seoul, Korea
J. Goh, T.J. Kim

Korea University, Seoul, Korea
S. Cho, S. Choi, Y. Go, D. Gyun, S. Ha, B. Hong, Y. Jo, Y. Kim, K. Lee, K.S. Lee, S. Lee, J. Lim, S.K. Park, Y. Roh

Seoul National University, Seoul, Korea
J. Almond, J. Kim, J.S. Kim, H. Lee, K. Lee, K. Nam, S.B. Oh, B.C. Radburn-Smith, S.h. Seo, U.K. Yang, H.D. Yoo, G.B. Yu

University of Seoul, Seoul, Korea
H. Kim, J.H. Kim, J.S.H. Lee, I.C. Park

Sungkyunkwan University, Suwon, Korea
Y. Choi, C. Hwang, J. Lee, I. Yu

Vilnius University, Vilnius, Lithuania
V. Dudenas, A. Juodagalvis, J. Vaitkus

National Centre for Particle Physics, Universiti Malaya, Kuala Lumpur, Malaysia
I. Ahmed, Z.A. Ibrahim, M.A.B. Md Ali[34], F. Mohamad Idris[35], W.A.T. Wan Abdullah, M.N. Yusli, Z. Zolkapli

Centro de Investigacion y de Estudios Avanzados del IPN, Mexico City, Mexico
Reyes-Almanza, R, Ramirez-Sanchez, G., Duran-Osuna, M. C., H. Castilla-Valdez, E. De La

Cruz-Burelo, I. Heredia-De La Cruz[36], Rabadan-Trejo, R. I., R. Lopez-Fernandez, J. Mejia Guisao, A. Sanchez-Hernandez

Universidad Iberoamericana, Mexico City, Mexico
S. Carrillo Moreno, C. Oropeza Barrera, F. Vazquez Valencia

Benemerita Universidad Autonoma de Puebla, Puebla, Mexico
J. Eysermans, I. Pedraza, H.A. Salazar Ibarguen, C. Uribe Estrada

Universidad Autónoma de San Luis Potosí, San Luis Potosí, Mexico
A. Morelos Pineda

University of Auckland, Auckland, New Zealand
D. Krofcheck

University of Canterbury, Christchurch, New Zealand
S. Bheesette, P.H. Butler

National Centre for Physics, Quaid-I-Azam University, Islamabad, Pakistan
A. Ahmad, M. Ahmad, Q. Hassan, H.R. Hoorani, A. Saddique, M.A. Shah, M. Shoaib, M. Waqas

National Centre for Nuclear Research, Swierk, Poland
H. Bialkowska, M. Bluj, B. Boimska, T. Frueboes, M. Górski, M. Kazana, K. Nawrocki, M. Szleper, P. Traczyk, P. Zalewski

Institute of Experimental Physics, Faculty of Physics, University of Warsaw, Warsaw, Poland
K. Bunkowski, A. Byszuk[37], K. Doroba, A. Kalinowski, M. Konecki, J. Krolikowski, M. Misiura, M. Olszewski, A. Pyskir, M. Walczak

Laboratório de Instrumentação e Física Experimental de Partículas, Lisboa, Portugal
P. Bargassa, C. Beirão Da Cruz E Silva, A. Di Francesco, P. Faccioli, B. Galinhas, M. Gallinaro, J. Hollar, N. Leonardo, L. Lloret Iglesias, M.V. Nemallapudi, J. Seixas, G. Strong, O. Toldaiev, D. Vadruccio, J. Varela

Joint Institute for Nuclear Research, Dubna, Russia
I. Golutvin, V. Karjavin, I. Kashunin, V. Korenkov, G. Kozlov, A. Lanev, A. Malakhov, V. Matveev[38,39], V.V. Mitsyn, P. Moisenz, V. Palichik, V. Perelygin, S. Shmatov, S. Shulha, V. Smirnov, V. Trofimov, B.S. Yuldashev[40], A. Zarubin, V. Zhiltsov

Petersburg Nuclear Physics Institute, Gatchina (St. Petersburg), Russia
Y. Ivanov, V. Kim[41], E. Kuznetsova[42], P. Levchenko, V. Murzin, V. Oreshkin, I. Smirnov, D. Sosnov, V. Sulimov, L. Uvarov, S. Vavilov, A. Vorobyev

Institute for Nuclear Research, Moscow, Russia
Yu. Andreev, A. Dermenev, S. Gninenko, N. Golubev, A. Karneyeu, M. Kirsanov, N. Krasnikov, A. Pashenkov, D. Tlisov, A. Toropin

Institute for Theoretical and Experimental Physics, Moscow, Russia
V. Epshteyn, V. Gavrilov, N. Lychkovskaya, V. Popov, I. Pozdnyakov, G. Safronov, A. Spiridonov, A. Stepennov, V. Stolin, M. Toms, E. Vlasov, A. Zhokin

Moscow Institute of Physics and Technology, Moscow, Russia
T. Aushev, A. Bylinkin[39]

National Research Nuclear University 'Moscow Engineering Physics Institute' (MEPhI), Moscow, Russia
M. Chadeeva[43], P. Parygin, D. Philippov, S. Polikarpov, E. Popova, V. Rusinov

P.N. Lebedev Physical Institute, Moscow, Russia
V. Andreev, M. Azarkin[39], I. Dremin[39], M. Kirakosyan[39], S.V. Rusakov, A. Terkulov

Skobeltsyn Institute of Nuclear Physics, Lomonosov Moscow State University, Moscow, Russia
A. Baskakov, A. Belyaev, E. Boos, M. Dubinin[44], L. Dudko, A. Ershov, A. Gribushin, V. Klyukhin, O. Kodolova, I. Lokhtin, I. Miagkov, S. Obraztsov, S. Petrushanko, V. Savrin, A. Snigirev

Novosibirsk State University (NSU), Novosibirsk, Russia
V. Blinov[45], D. Shtol[45], Y. Skovpen[45]

State Research Center of Russian Federation, Institute for High Energy Physics of NRC "Kurchatov Institute", Protvino, Russia
I. Azhgirey, I. Bayshev, S. Bitioukov, D. Elumakhov, A. Godizov, V. Kachanov, A. Kalinin, D. Konstantinov, P. Mandrik, V. Petrov, R. Ryutin, A. Sobol, S. Troshin, N. Tyurin, A. Uzunian, A. Volkov

National Research Tomsk Polytechnic University, Tomsk, Russia
A. Babaev

University of Belgrade, Faculty of Physics and Vinca Institute of Nuclear Sciences, Belgrade, Serbia
P. Adzic[46], P. Cirkovic, D. Devetak, M. Dordevic, J. Milosevic

Centro de Investigaciones Energéticas Medioambientales y Tecnológicas (CIEMAT), Madrid, Spain
J. Alcaraz Maestre, I. Bachiller, M. Barrio Luna, J.A. Brochero Cifuentes, M. Cerrada, N. Colino, B. De La Cruz, A. Delgado Peris, C. Fernandez Bedoya, J.P. Fernández Ramos, J. Flix, M.C. Fouz, O. Gonzalez Lopez, S. Goy Lopez, J.M. Hernandez, M.I. Josa, D. Moran, A. Pérez-Calero Yzquierdo, J. Puerta Pelayo, I. Redondo, L. Romero, M.S. Soares, A. Triossi, A. Álvarez Fernández

Universidad Autónoma de Madrid, Madrid, Spain
C. Albajar, J.F. de Trocóniz

Universidad de Oviedo, Oviedo, Spain
J. Cuevas, C. Erice, J. Fernandez Menendez, S. Folgueras, I. Gonzalez Caballero, J.R. González Fernández, E. Palencia Cortezon, S. Sanchez Cruz, P. Vischia, J.M. Vizan Garcia

Instituto de Física de Cantabria (IFCA), CSIC-Universidad de Cantabria, Santander, Spain
I.J. Cabrillo, A. Calderon, B. Chazin Quero, J. Duarte Campderros, M. Fernandez, P.J. Fernández Manteca, J. Garcia-Ferrero, A. García Alonso, G. Gomez, A. Lopez Virto, J. Marco, C. Martinez Rivero, P. Martinez Ruiz del Arbol, F. Matorras, J. Piedra Gomez, C. Prieels, T. Rodrigo, A. Ruiz-Jimeno, L. Scodellaro, N. Trevisani, I. Vila, R. Vilar Cortabitarte

CERN, European Organization for Nuclear Research, Geneva, Switzerland
D. Abbaneo, B. Akgun, E. Auffray, P. Baillon, A.H. Ball, D. Barney, J. Bendavid, M. Bianco, A. Bocci, C. Botta, T. Camporesi, M. Cepeda, G. Cerminara, E. Chapon, Y. Chen, D. d'Enterria, A. Dabrowski, V. Daponte, A. David, M. De Gruttola, A. De Roeck, N. Deelen, M. Dobson, T. du Pree, M. Dünser, N. Dupont, A. Elliott-Peisert, P. Everaerts, F. Fallavollita[47], G. Franzoni, J. Fulcher, W. Funk, D. Gigi, A. Gilbert, K. Gill, F. Glege, D. Gulhan, J. Hegeman, V. Innocente, A. Jafari, P. Janot, O. Karacheban[20], J. Kieseler, V. Knünz, A. Kornmayer, M. Krammer[1], C. Lange, P. Lecoq, C. Lourenço, M.T. Lucchini, L. Malgeri, M. Mannelli, A. Martelli, F. Meijers,

J.A. Merlin, S. Mersi, E. Meschi, P. Milenovic[48], F. Moortgat, M. Mulders, H. Neugebauer, J. Ngadiuba, S. Orfanelli, L. Orsini, F. Pantaleo[17], L. Pape, E. Perez, M. Peruzzi, A. Petrilli, G. Petrucciani, A. Pfeiffer, M. Pierini, F.M. Pitters, D. Rabady, A. Racz, T. Reis, G. Rolandi[49], M. Rovere, H. Sakulin, C. Schäfer, C. Schwick, M. Seidel, M. Selvaggi, A. Sharma, P. Silva, P. Sphicas[50], A. Stakia, J. Steggemann, M. Stoye, M. Tosi, D. Treille, A. Tsirou, V. Veckalns[51], M. Verweij, W.D. Zeuner

Paul Scherrer Institut, Villigen, Switzerland
W. Bertl†, L. Caminada[52], K. Deiters, W. Erdmann, R. Horisberger, Q. Ingram, H.C. Kaestli, D. Kotlinski, U. Langenegger, T. Rohe, S.A. Wiederkehr

ETH Zurich - Institute for Particle Physics and Astrophysics (IPA), Zurich, Switzerland
M. Backhaus, L. Bäni, P. Berger, B. Casal, N. Chernyavskaya, G. Dissertori, M. Dittmar, M. Donegà, C. Dorfer, C. Grab, C. Heidegger, D. Hits, J. Hoss, T. Klijnsma, W. Lustermann, M. Marionneau, M.T. Meinhard, D. Meister, F. Micheli, P. Musella, F. Nessi-Tedaldi, J. Pata, F. Pauss, G. Perrin, L. Perrozzi, M. Quittnat, M. Reichmann, D. Ruini, D.A. Sanz Becerra, M. Schönenberger, L. Shchutska, V.R. Tavolaro, K. Theofilatos, M.L. Vesterbacka Olsson, R. Wallny, D.H. Zhu

Universität Zürich, Zurich, Switzerland
T.K. Aarrestad, C. Amsler[53], D. Brzhechko, M.F. Canelli, A. De Cosa, R. Del Burgo, S. Donato, C. Galloni, T. Hreus, B. Kilminster, I. Neutelings, D. Pinna, G. Rauco, P. Robmann, D. Salerno, K. Schweiger, C. Seitz, Y. Takahashi, A. Zucchetta

National Central University, Chung-Li, Taiwan
Y.H. Chang, K.y. Cheng, T.H. Doan, Sh. Jain, R. Khurana, C.M. Kuo, W. Lin, A. Pozdnyakov, S.S. Yu

National Taiwan University (NTU), Taipei, Taiwan
Arun Kumar, P. Chang, Y. Chao, K.F. Chen, P.H. Chen, F. Fiori, W.-S. Hou, Y. Hsiung, Y.F. Liu, R.-S. Lu, E. Paganis, A. Psallidas, A. Steen, J.f. Tsai

Chulalongkorn University, Faculty of Science, Department of Physics, Bangkok, Thailand
B. Asavapibhop, K. Kovitanggoon, G. Singh, N. Srimanobhas

Çukurova University, Physics Department, Science and Art Faculty, Adana, Turkey
A. Bat, F. Boran, S. Cerci[54], S. Damarseckin, Z.S. Demiroglu, C. Dozen, I. Dumanoglu, S. Girgis, G. Gokbulut, Y. Guler, I. Hos[55], E.E. Kangal[56], O. Kara, A. Kayis Topaksu, U. Kiminsu, M. Oglakci, G. Onengut, K. Ozdemir[57], D. Sunar Cerci[54], B. Tali[54], U.G. Tok, S. Turkcapar, I.S. Zorbakir, C. Zorbilmez

Middle East Technical University, Physics Department, Ankara, Turkey
G. Karapinar[58], K. Ocalan[59], M. Yalvac, M. Zeyrek

Bogazici University, Istanbul, Turkey
I.O. Atakisi, E. Gülmez, M. Kaya[60], O. Kaya[61], S. Tekten, E.A. Yetkin[62]

Istanbul Technical University, Istanbul, Turkey
M.N. Agaras, S. Atay, A. Cakir, K. Cankocak, Y. Komurcu

Institute for Scintillation Materials of National Academy of Science of Ukraine, Kharkov, Ukraine
B. Grynyov

National Scientific Center, Kharkov Institute of Physics and Technology, Kharkov, Ukraine
L. Levchuk

University of Bristol, Bristol, United Kingdom
F. Ball, L. Beck, J.J. Brooke, D. Burns, E. Clement, D. Cussans, O. Davignon, H. Flacher, J. Goldstein, G.P. Heath, H.F. Heath, L. Kreczko, D.M. Newbold[63], S. Paramesvaran, T. Sakuma, S. Seif El Nasr-storey, D. Smith, V.J. Smith

Rutherford Appleton Laboratory, Didcot, United Kingdom
K.W. Bell, A. Belyaev[64], C. Brew, R.M. Brown, D. Cieri, D.J.A. Cockerill, J.A. Coughlan, K. Harder, S. Harper, J. Linacre, E. Olaiya, D. Petyt, C.H. Shepherd-Themistocleous, A. Thea, I.R. Tomalin, T. Williams, W.J. Womersley

Imperial College, London, United Kingdom
G. Auzinger, R. Bainbridge, P. Bloch, J. Borg, S. Breeze, O. Buchmuller, A. Bundock, S. Casasso, D. Colling, L. Corpe, P. Dauncey, G. Davies, M. Della Negra, R. Di Maria, Y. Haddad, G. Hall, G. Iles, T. James, M. Komm, R. Lane, C. Laner, L. Lyons, A.-M. Magnan, S. Malik, L. Mastrolorenzo, T. Matsushita, J. Nash[65], A. Nikitenko[7], V. Palladino, M. Pesaresi, A. Richards, A. Rose, E. Scott, C. Seez, A. Shtipliyski, T. Strebler, S. Summers, A. Tapper, K. Uchida, M. Vazquez Acosta[66], T. Virdee[17], N. Wardle, D. Winterbottom, J. Wright, S.C. Zenz

Brunel University, Uxbridge, United Kingdom
J.E. Cole, P.R. Hobson, A. Khan, P. Kyberd, C.K. Mackay, A. Morton, I.D. Reid, L. Teodorescu, S. Zahid

Baylor University, Waco, USA
A. Borzou, K. Call, J. Dittmann, K. Hatakeyama, H. Liu, N. Pastika, C. Smith

Catholic University of America, Washington DC, USA
R. Bartek, A. Dominguez

The University of Alabama, Tuscaloosa, USA
A. Buccilli, S.I. Cooper, C. Henderson, P. Rumerio, C. West

Boston University, Boston, USA
D. Arcaro, A. Avetisyan, T. Bose, D. Gastler, D. Rankin, C. Richardson, J. Rohlf, L. Sulak, D. Zou

Brown University, Providence, USA
G. Benelli, D. Cutts, M. Hadley, J. Hakala, U. Heintz, J.M. Hogan[67], K.H.M. Kwok, E. Laird, G. Landsberg, J. Lee, Z. Mao, M. Narain, J. Pazzini, S. Piperov, S. Sagir, R. Syarif, D. Yu

University of California, Davis, Davis, USA
R. Band, C. Brainerd, R. Breedon, D. Burns, M. Calderon De La Barca Sanchez, M. Chertok, J. Conway, R. Conway, P.T. Cox, R. Erbacher, C. Flores, G. Funk, W. Ko, R. Lander, C. Mclean, M. Mulhearn, D. Pellett, J. Pilot, S. Shalhout, M. Shi, J. Smith, D. Stolp, D. Taylor, K. Tos, M. Tripathi, Z. Wang, F. Zhang

University of California, Los Angeles, USA
M. Bachtis, C. Bravo, R. Cousins, A. Dasgupta, A. Florent, J. Hauser, M. Ignatenko, N. Mccoll, S. Regnard, D. Saltzberg, C. Schnaible, V. Valuev

University of California, Riverside, Riverside, USA
E. Bouvier, K. Burt, R. Clare, J. Ellison, J.W. Gary, S.M.A. Ghiasi Shirazi, G. Hanson, G. Karapostoli, E. Kennedy, F. Lacroix, O.R. Long, M. Olmedo Negrete, M.I. Paneva, W. Si, L. Wang, H. Wei, S. Wimpenny, B. R. Yates

University of California, San Diego, La Jolla, USA
J.G. Branson, S. Cittolin, M. Derdzinski, R. Gerosa, D. Gilbert, B. Hashemi, A. Holzner, D. Klein, G. Kole, V. Krutelyov, J. Letts, M. Masciovecchio, D. Olivito, S. Padhi, M. Pieri, M. Sani, V. Sharma, S. Simon, M. Tadel, A. Vartak, S. Wasserbaech[68], J. Wood, F. Würthwein, A. Yagil, G. Zevi Della Porta

University of California, Santa Barbara - Department of Physics, Santa Barbara, USA
N. Amin, R. Bhandari, J. Bradmiller-Feld, C. Campagnari, M. Citron, A. Dishaw, V. Dutta, M. Franco Sevilla, L. Gouskos, R. Heller, J. Incandela, A. Ovcharova, H. Qu, J. Richman, D. Stuart, I. Suarez, J. Yoo

California Institute of Technology, Pasadena, USA
D. Anderson, A. Bornheim, J. Bunn, J.M. Lawhorn, H.B. Newman, T. Q. Nguyen, C. Pena, M. Spiropulu, J.R. Vlimant, R. Wilkinson, S. Xie, Z. Zhang, R.Y. Zhu

Carnegie Mellon University, Pittsburgh, USA
M.B. Andrews, T. Ferguson, T. Mudholkar, M. Paulini, J. Russ, M. Sun, H. Vogel, I. Vorobiev, M. Weinberg

University of Colorado Boulder, Boulder, USA
J.P. Cumalat, W.T. Ford, F. Jensen, A. Johnson, M. Krohn, S. Leontsinis, E. MacDonald, T. Mulholland, K. Stenson, K.A. Ulmer, S.R. Wagner

Cornell University, Ithaca, USA
J. Alexander, J. Chaves, Y. Cheng, J. Chu, A. Datta, K. Mcdermott, N. Mirman, J.R. Patterson, D. Quach, A. Rinkevicius, A. Ryd, L. Skinnari, L. Soffi, S.M. Tan, Z. Tao, J. Thom, J. Tucker, P. Wittich, M. Zientek

Fermi National Accelerator Laboratory, Batavia, USA
S. Abdullin, M. Albrow, M. Alyari, G. Apollinari, A. Apresyan, A. Apyan, S. Banerjee, L.A.T. Bauerdick, A. Beretvas, J. Berryhill, P.C. Bhat, G. Bolla[†], K. Burkett, J.N. Butler, A. Canepa, G.B. Cerati, H.W.K. Cheung, F. Chlebana, M. Cremonesi, J. Duarte, V.D. Elvira, J. Freeman, Z. Gecse, E. Gottschalk, L. Gray, D. Green, S. Grünendahl, O. Gutsche, J. Hanlon, R.M. Harris, S. Hasegawa, J. Hirschauer, Z. Hu, B. Jayatilaka, S. Jindariani, M. Johnson, U. Joshi, B. Klima, M.J. Kortelainen, B. Kreis, S. Lammel, D. Lincoln, R. Lipton, M. Liu, T. Liu, R. Lopes De Sá, J. Lykken, K. Maeshima, N. Magini, J.M. Marraffino, D. Mason, P. McBride, P. Merkel, S. Mrenna, S. Nahn, V. O'Dell, K. Pedro, O. Prokofyev, G. Rakness, L. Ristori, A. Savoy-Navarro[69], B. Schneider, E. Sexton-Kennedy, A. Soha, W.J. Spalding, L. Spiegel, S. Stoynev, J. Strait, N. Strobbe, L. Taylor, S. Tkaczyk, N.V. Tran, L. Uplegger, E.W. Vaandering, C. Vernieri, M. Verzocchi, R. Vidal, M. Wang, H.A. Weber, A. Whitbeck, W. Wu

University of Florida, Gainesville, USA
D. Acosta, P. Avery, P. Bortignon, D. Bourilkov, A. Brinkerhoff, A. Carnes, M. Carver, D. Curry, R.D. Field, I.K. Furic, S.V. Gleyzer, B.M. Joshi, J. Konigsberg, A. Korytov, K. Kotov, P. Ma, K. Matchev, H. Mei, G. Mitselmakher, K. Shi, D. Sperka, N. Terentyev, L. Thomas, J. Wang, S. Wang, J. Yelton

Florida International University, Miami, USA
Y.R. Joshi, S. Linn, P. Markowitz, J.L. Rodriguez

Florida State University, Tallahassee, USA
A. Ackert, T. Adams, A. Askew, S. Hagopian, V. Hagopian, K.F. Johnson, T. Kolberg, G. Martinez, T. Perry, H. Prosper, A. Saha, A. Santra, V. Sharma, R. Yohay

Florida Institute of Technology, Melbourne, USA
M.M. Baarmand, V. Bhopatkar, S. Colafranceschi, M. Hohlmann, D. Noonan, T. Roy, F. Yumiceva

University of Illinois at Chicago (UIC), Chicago, USA
M.R. Adams, L. Apanasevich, D. Berry, R.R. Betts, R. Cavanaugh, X. Chen, S. Dittmer, O. Evdokimov, C.E. Gerber, D.A. Hangal, D.J. Hofman, K. Jung, J. Kamin, C. Mills, I.D. Sandoval Gonzalez, M.B. Tonjes, N. Varelas, H. Wang, Z. Wu, J. Zhang

The University of Iowa, Iowa City, USA
B. Bilki[70], W. Clarida, K. Dilsiz[71], S. Durgut, R.P. Gandrajula, M. Haytmyradov, V. Khristenko, J.-P. Merlo, H. Mermerkaya[72], A. Mestvirishvili, A. Moeller, J. Nachtman, H. Ogul[73], Y. Onel, F. Ozok[74], A. Penzo, C. Snyder, E. Tiras, J. Wetzel, K. Yi

Johns Hopkins University, Baltimore, USA
B. Blumenfeld, A. Cocoros, N. Eminizer, D. Fehling, L. Feng, A.V. Gritsan, W.T. Hung, P. Maksimovic, J. Roskes, U. Sarica, M. Swartz, M. Xiao, C. You

The University of Kansas, Lawrence, USA
A. Al-bataineh, P. Baringer, A. Bean, J.F. Benitez, S. Boren, J. Bowen, J. Castle, S. Khalil, A. Kropivnitskaya, D. Majumder, W. Mcbrayer, M. Murray, C. Rogan, C. Royon, S. Sanders, E. Schmitz, J.D. Tapia Takaki, Q. Wang

Kansas State University, Manhattan, USA
A. Ivanov, K. Kaadze, Y. Maravin, A. Modak, A. Mohammadi, L.K. Saini, N. Skhirtladze

Lawrence Livermore National Laboratory, Livermore, USA
F. Rebassoo, D. Wright

University of Maryland, College Park, USA
A. Baden, O. Baron, A. Belloni, S.C. Eno, Y. Feng, C. Ferraioli, N.J. Hadley, S. Jabeen, G.Y. Jeng, R.G. Kellogg, J. Kunkle, A.C. Mignerey, F. Ricci-Tam, Y.H. Shin, A. Skuja, S.C. Tonwar

Massachusetts Institute of Technology, Cambridge, USA
D. Abercrombie, B. Allen, V. Azzolini, R. Barbieri, A. Baty, G. Bauer, R. Bi, S. Brandt, W. Busza, I.A. Cali, M. D'Alfonso, Z. Demiragli, G. Gomez Ceballos, M. Goncharov, P. Harris, D. Hsu, M. Hu, Y. Iiyama, G.M. Innocenti, M. Klute, D. Kovalskyi, Y.-J. Lee, A. Levin, P.D. Luckey, B. Maier, A.C. Marini, C. Mcginn, C. Mironov, S. Narayanan, X. Niu, C. Paus, C. Roland, G. Roland, G.S.F. Stephans, K. Sumorok, K. Tatar, D. Velicanu, J. Wang, T.W. Wang, B. Wyslouch, S. Zhaozhong

University of Minnesota, Minneapolis, USA
A.C. Benvenuti, R.M. Chatterjee, A. Evans, P. Hansen, S. Kalafut, Y. Kubota, Z. Lesko, J. Mans, S. Nourbakhsh, N. Ruckstuhl, R. Rusack, J. Turkewitz, M.A. Wadud

University of Mississippi, Oxford, USA
J.G. Acosta, S. Oliveros

University of Nebraska-Lincoln, Lincoln, USA
E. Avdeeva, K. Bloom, D.R. Claes, C. Fangmeier, F. Golf, R. Gonzalez Suarez, R. Kamalieddin, I. Kravchenko, J. Monroy, J.E. Siado, G.R. Snow, B. Stieger

State University of New York at Buffalo, Buffalo, USA
A. Godshalk, C. Harrington, I. Iashvili, D. Nguyen, A. Parker, S. Rappoccio, B. Roozbahani

Northeastern University, Boston, USA
G. Alverson, E. Barberis, C. Freer, A. Hortiangtham, A. Massironi, D.M. Morse, T. Orimoto, R. Teixeira De Lima, T. Wamorkar, B. Wang, A. Wisecarver, D. Wood

Northwestern University, Evanston, USA
S. Bhattacharya, O. Charaf, K.A. Hahn, N. Mucia, N. Odell, M.H. Schmitt, K. Sung, M. Trovato, M. Velasco

University of Notre Dame, Notre Dame, USA
R. Bucci, N. Dev, M. Hildreth, K. Hurtado Anampa, C. Jessop, D.J. Karmgard, N. Kellams, K. Lannon, W. Li, N. Loukas, N. Marinelli, F. Meng, C. Mueller, Y. Musienko[38], M. Planer, A. Reinsvold, R. Ruchti, P. Siddireddy, G. Smith, S. Taroni, M. Wayne, A. Wightman, M. Wolf, A. Woodard

The Ohio State University, Columbus, USA
J. Alimena, L. Antonelli, B. Bylsma, L.S. Durkin, S. Flowers, B. Francis, A. Hart, C. Hill, W. Ji, T.Y. Ling, W. Luo, B.L. Winer, H.W. Wulsin

Princeton University, Princeton, USA
S. Cooperstein, O. Driga, P. Elmer, J. Hardenbrook, P. Hebda, S. Higginbotham, A. Kalogeropoulos, D. Lange, J. Luo, D. Marlow, K. Mei, I. Ojalvo, J. Olsen, C. Palmer, P. Piroué, J. Salfeld-Nebgen, D. Stickland, C. Tully

University of Puerto Rico, Mayaguez, USA
S. Malik, S. Norberg

Purdue University, West Lafayette, USA
A. Barker, V.E. Barnes, S. Das, L. Gutay, M. Jones, A.W. Jung, A. Khatiwada, D.H. Miller, N. Neumeister, C.C. Peng, H. Qiu, J.F. Schulte, J. Sun, F. Wang, R. Xiao, W. Xie

Purdue University Northwest, Hammond, USA
T. Cheng, J. Dolen, N. Parashar

Rice University, Houston, USA
Z. Chen, K.M. Ecklund, S. Freed, F.J.M. Geurts, M. Guilbaud, M. Kilpatrick, W. Li, B. Michlin, B.P. Padley, J. Roberts, J. Rorie, W. Shi, Z. Tu, J. Zabel, A. Zhang

University of Rochester, Rochester, USA
A. Bodek, P. de Barbaro, R. Demina, Y.t. Duh, T. Ferbel, M. Galanti, A. Garcia-Bellido, J. Han, O. Hindrichs, A. Khukhunaishvili, K.H. Lo, P. Tan, M. Verzetti

The Rockefeller University, New York, USA
R. Ciesielski, K. Goulianos, C. Mesropian

Rutgers, The State University of New Jersey, Piscataway, USA
A. Agapitos, J.P. Chou, Y. Gershtein, T.A. Gómez Espinosa, E. Halkiadakis, M. Heindl, E. Hughes, S. Kaplan, R. Kunnawalkam Elayavalli, S. Kyriacou, A. Lath, R. Montalvo, K. Nash, M. Osherson, H. Saka, S. Salur, S. Schnetzer, D. Sheffield, S. Somalwar, R. Stone, S. Thomas, P. Thomassen, M. Walker

University of Tennessee, Knoxville, USA
A.G. Delannoy, J. Heideman, G. Riley, K. Rose, S. Spanier, K. Thapa

Texas A&M University, College Station, USA
O. Bouhali[75], A. Castaneda Hernandez[75], A. Celik, M. Dalchenko, M. De Mattia, A. Delgado,

S. Dildick, R. Eusebi, J. Gilmore, T. Huang, T. Kamon[76], R. Mueller, Y. Pakhotin, R. Patel, A. Perloff, L. Perniè, D. Rathjens, A. Safonov, A. Tatarinov

Texas Tech University, Lubbock, USA
N. Akchurin, J. Damgov, F. De Guio, P.R. Dudero, J. Faulkner, E. Gurpinar, S. Kunori, K. Lamichhane, S.W. Lee, T. Mengke, S. Muthumuni, T. Peltola, S. Undleeb, I. Volobouev, Z. Wang

Vanderbilt University, Nashville, USA
S. Greene, A. Gurrola, R. Janjam, W. Johns, C. Maguire, A. Melo, H. Ni, K. Padeken, J.D. Ruiz Alvarez, P. Sheldon, S. Tuo, J. Velkovska, Q. Xu

University of Virginia, Charlottesville, USA
M.W. Arenton, P. Barria, B. Cox, R. Hirosky, M. Joyce, A. Ledovskoy, H. Li, C. Neu, T. Sinthuprasith, Y. Wang, E. Wolfe, F. Xia

Wayne State University, Detroit, USA
R. Harr, P.E. Karchin, N. Poudyal, J. Sturdy, P. Thapa, S. Zaleski

University of Wisconsin - Madison, Madison, WI, USA
M. Brodski, J. Buchanan, C. Caillol, D. Carlsmith, S. Dasu, L. Dodd, S. Duric, B. Gomber, M. Grothe, M. Herndon, A. Hervé, U. Hussain, P. Klabbers, A. Lanaro, A. Levine, K. Long, R. Loveless, V. Rekovic, T. Ruggles, A. Savin, N. Smith, W.H. Smith, N. Woods

†: Deceased
1: Also at Vienna University of Technology, Vienna, Austria
2: Also at IRFU, CEA, Université Paris-Saclay, Gif-sur-Yvette, France
3: Also at Universidade Estadual de Campinas, Campinas, Brazil
4: Also at Federal University of Rio Grande do Sul, Porto Alegre, Brazil
5: Also at Universidade Federal de Pelotas, Pelotas, Brazil
6: Also at Université Libre de Bruxelles, Bruxelles, Belgium
7: Also at Institute for Theoretical and Experimental Physics, Moscow, Russia
8: Also at Joint Institute for Nuclear Research, Dubna, Russia
9: Also at Zewail City of Science and Technology, Zewail, Egypt
10: Now at Fayoum University, El-Fayoum, Egypt
11: Also at British University in Egypt, Cairo, Egypt
12: Now at Ain Shams University, Cairo, Egypt
13: Also at Department of Physics, King Abdulaziz University, Jeddah, Saudi Arabia
14: Also at Université de Haute Alsace, Mulhouse, France
15: Also at Skobeltsyn Institute of Nuclear Physics, Lomonosov Moscow State University, Moscow, Russia
16: Also at Tbilisi State University, Tbilisi, Georgia
17: Also at CERN, European Organization for Nuclear Research, Geneva, Switzerland
18: Also at RWTH Aachen University, III. Physikalisches Institut A, Aachen, Germany
19: Also at University of Hamburg, Hamburg, Germany
20: Also at Brandenburg University of Technology, Cottbus, Germany
21: Also at Institute of Nuclear Research ATOMKI, Debrecen, Hungary
22: Also at Institute of Physics, University of Debrecen, Debrecen, Hungary
23: Also at MTA-ELTE Lendület CMS Particle and Nuclear Physics Group, Eötvös Loránd University, Budapest, Hungary
24: Also at Indian Institute of Technology Bhubaneswar, Bhubaneswar, India
25: Also at Institute of Physics, Bhubaneswar, India

26: Also at Shoolini University, Solan, India
27: Also at University of Visva-Bharati, Santiniketan, India
28: Also at University of Ruhuna, Matara, Sri Lanka
29: Also at Isfahan University of Technology, Isfahan, Iran
30: Also at Yazd University, Yazd, Iran
31: Also at Plasma Physics Research Center, Science and Research Branch, Islamic Azad University, Tehran, Iran
32: Also at Università degli Studi di Siena, Siena, Italy
33: Also at INFN Sezione di Milano-Bicocca; Università di Milano-Bicocca, Milano, Italy
34: Also at International Islamic University of Malaysia, Kuala Lumpur, Malaysia
35: Also at Malaysian Nuclear Agency, MOSTI, Kajang, Malaysia
36: Also at Consejo Nacional de Ciencia y Tecnología, Mexico city, Mexico
37: Also at Warsaw University of Technology, Institute of Electronic Systems, Warsaw, Poland
38: Also at Institute for Nuclear Research, Moscow, Russia
39: Now at National Research Nuclear University 'Moscow Engineering Physics Institute' (MEPhI), Moscow, Russia
40: Also at Institute of Nuclear Physics of the Uzbekistan Academy of Sciences, Tashkent, Uzbekistan
41: Also at St. Petersburg State Polytechnical University, St. Petersburg, Russia
42: Also at University of Florida, Gainesville, USA
43: Also at P.N. Lebedev Physical Institute, Moscow, Russia
44: Also at California Institute of Technology, Pasadena, USA
45: Also at Budker Institute of Nuclear Physics, Novosibirsk, Russia
46: Also at Faculty of Physics, University of Belgrade, Belgrade, Serbia
47: Also at INFN Sezione di Pavia; Università di Pavia, Pavia, Italy
48: Also at University of Belgrade, Faculty of Physics and Vinca Institute of Nuclear Sciences, Belgrade, Serbia
49: Also at Scuola Normale e Sezione dell'INFN, Pisa, Italy
50: Also at National and Kapodistrian University of Athens, Athens, Greece
51: Also at Riga Technical University, Riga, Latvia
52: Also at Universität Zürich, Zurich, Switzerland
53: Also at Stefan Meyer Institute for Subatomic Physics (SMI), Vienna, Austria
54: Also at Adiyaman University, Adiyaman, Turkey
55: Also at Istanbul Aydin University, Istanbul, Turkey
56: Also at Mersin University, Mersin, Turkey
57: Also at Piri Reis University, Istanbul, Turkey
58: Also at Izmir Institute of Technology, Izmir, Turkey
59: Also at Necmettin Erbakan University, Konya, Turkey
60: Also at Marmara University, Istanbul, Turkey
61: Also at Kafkas University, Kars, Turkey
62: Also at Istanbul Bilgi University, Istanbul, Turkey
63: Also at Rutherford Appleton Laboratory, Didcot, United Kingdom
64: Also at School of Physics and Astronomy, University of Southampton, Southampton, United Kingdom
65: Also at Monash University, Faculty of Science, Clayton, Australia
66: Also at Instituto de Astrofísica de Canarias, La Laguna, Spain
67: Also at Bethel University, St. Paul, USA
68: Also at Utah Valley University, Orem, USA
69: Also at Purdue University, West Lafayette, USA

70: Also at Beykent University, Istanbul, Turkey
71: Also at Bingol University, Bingol, Turkey
72: Also at Erzincan University, Erzincan, Turkey
73: Also at Sinop University, Sinop, Turkey
74: Also at Mimar Sinan University, Istanbul, Istanbul, Turkey
75: Also at Texas A&M University at Qatar, Doha, Qatar
76: Also at Kyungpook National University, Daegu, Korea